

PREPARED FOR SUBMISSION TO JHEP

Phase transitions in the early universe

Marieke Postma^a

^aNikhef, Theory Group, Science Park 105, 1098 XG, Amsterdam, The Netherlands

E-mail: mpostma@nikhef.nl

ABSTRACT: Lecture notes on phase transitions in the early universe.

Contents

1	Introduction	1
2	Thermal corrections to the potential	3
2.1	KMS relation	3
2.2	Real scalar field	5
2.2.1	QM at zero temperature	5
2.2.2	QM at finite temperature	6
2.2.3	QFT at finite temperature	6
2.3	Breakdown of thermal perturbation theory	8
2.4	Excercises	9
2.4.1	Excercise: Equilibrium dynamics	9
2.4.2	Excercise: Summation over bosonic Matsubara frequencies	9
3	Thermal corrections to the SM Higgs potential and order of the PT	10
3.1	Excercises	13
3.1.1	Excercise: Allowed modifications to the Higgs potential	13
3.1.2	Excercise: Higgs-singlet model	14
4	Tunneling and bubble nucleation	14
4.1	QM at zero temperature	14
4.2	QFT	16
4.3	Bubble nucleation at finite temperature	16
4.3.1	Nucleation temperature	17
4.3.2	Thin wall approximation	18
4.3.3	Thick wall approximation	19
4.4	Fate of the false vacuum	20
4.5	Excercises	20
4.5.1	Excercise: thin wall solution	20
4.5.2	Excercise: thick wall regime	21
5	Electroweak baryogenesis	21
5.1	Sakharov conditions and EW baryogenesis	22
5.1.1	Sphalerons	23
5.2	EW baryogenesis	25
5.3	Constraints from electric dipole moment measurements	28
5.4	Excercises	31
5.4.1	Excercise: sphaleron rate	31
5.4.2	Excercise: Dirac equation	31

5.4.3	Excercise:Magnetic moment of a Dirac fermion	31
6	Gravitational waves	31
6.1	GW from 1st order PT	34
6.2	Excercises	37
6.2.1	Excercise: Energy momentum conservation	37
A	FLWR cosmology	37
A.1	Friedmann equation	38
A.2	Thermal history	40

1 Introduction

Particle cosmology has two main goals: 1) find a microphysics description/understanding of the universe, and 2) use the extreme conditions in the universe as a test bed for particle physics. Need observations to test theories.

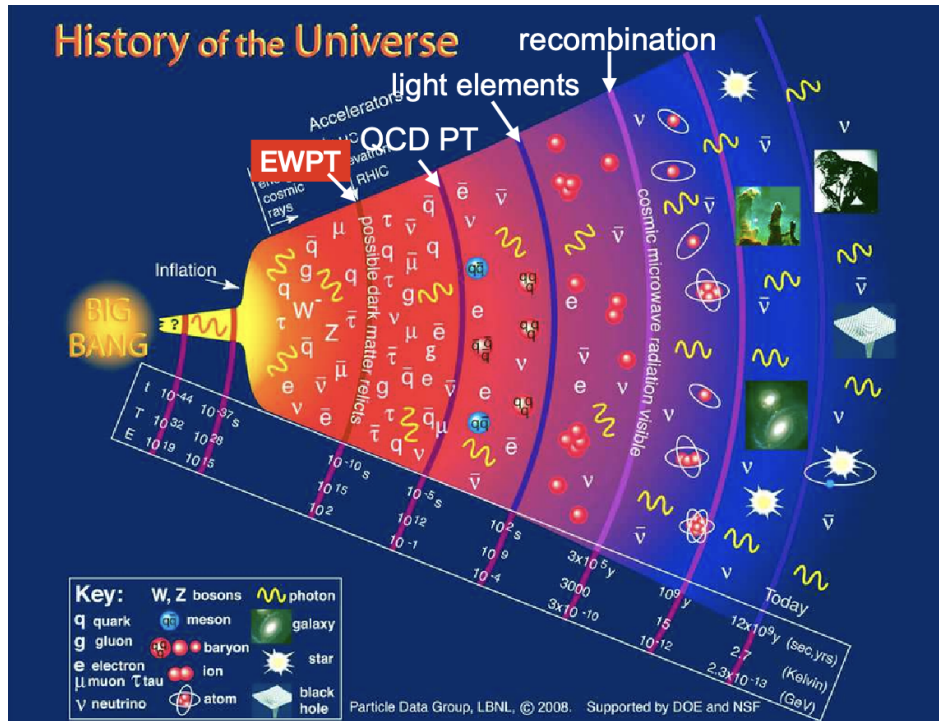


Figure 1. Timeline of the universe.

During most of its history the universe expansion was adiabatic, with all processes near equilibrium. Almost all of the interesting physics that leave traces in today's universe happened at the instances when the evolution of the universe was non-adiabatic. For example

- Recombination at $T \sim \text{eV}$ or $t \sim 300.00 \text{ yrs}$. Ions and electrons combined into neutral atoms, and the plasma became transparent to light. Since this time, photons can travel unscattered to us today (13.8 billion yrs after the big bang). This is the cosmic microwave background (CMB).
- Big bang nucleosynthesis (BBN) at $T \sim \text{MeV}$ or $t \sim 3 \text{ minutes}$. As the temperature dropped below the binding energy of deuterium, the light elements (deuterium, helium, lithium) started to form. One can observe their primordial abundances in today's universe.
- QCD phase transition (PT) at $T \sim 100 \text{ MeV}$ or $t \sim 10^{-5} \text{ s}$ ($10 \mu\text{s}$). Quarks confine into mesons and baryons.
- electroweak (EW) PT at $T \sim 100 \text{ GeV}$ or $t \sim 10^{-10} \text{ s}$ ($10 \eta\text{s}$). The EW symmetry is broken by the Higgs mechanism, and gauge bosons and fermions obtain masses.

If PTs are sufficiently abrupt/out of equilibrium, they can leave traces in today's universe: gravitational waves, magnetic fields, baryogenesis, PBH formation.

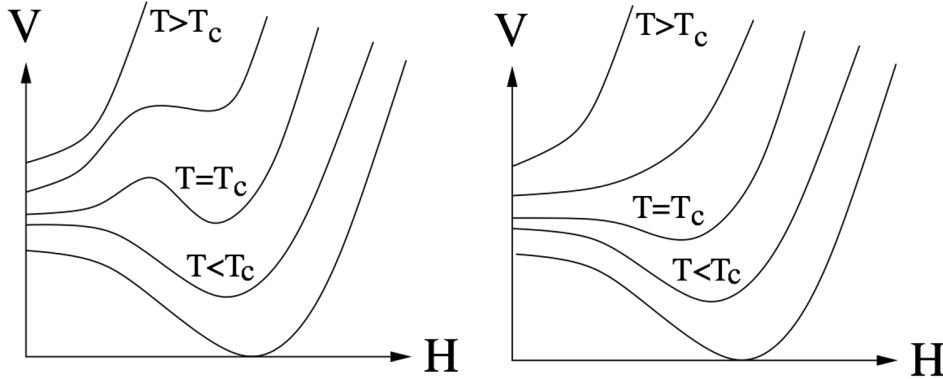


Figure 2. Potential for 1st and 2nd order/crossover PT. For 1st order PT the order parameter changes discontinuously, and PT proceeds via bubble nucleation.

PT: change of the physical state (phase) of a system due to changing external conditions (e.g. T , B , ...) described in terms of an order parameter. More formal: point at which the free energy of the system is non-analytic. The order parameter of the EWPT can be taken as the Higgs vev $\langle H^\dagger H \rangle$ which breaks the EW symmetry $SU(2) \times Y(1)_Y \rightarrow U(1)_Q$; the order parameter of the QCD PT is the quark bilinear $\langle \bar{q}_R q_L \rangle$ which breaks the global flavor symmetry $SU_L(N_f) \times SU_R(N_f) \rightarrow SU_V(N_f)$.

The EW potential at zero temperature is the Mexican hat potential. The classical tree-level potential gets corrected by quantum corrections. When calculated in the presence of a thermal bath (and not vacuum) loop particles can exchange energy with the plasma (there are now quantum and thermal fluctuations), and the corrections become temperature dependent. At high temperature the effect is that the symmetry is restored. The order of the PT depends

on the zero temperature potential and on thermal corrections. For cosmology, a 1st order PT is most interesting, as the dynamics of bubble formation and coalescence is far from equilibrium, and thus may leave observable traces.

Plan of the lectures

- Potential V at finite temperature.
- Decay rate of the false vacuum and bubble nucleation.
- EW baryogenesis.
- Other probes: Gravitational waves, stability of Higgs potential.

2 Thermal corrections to the potential

Further reading: book on thermal field theory [1], lecture notes on thermal field theory [2] and on thermal field theory and the effective potential [3]. We will consider the one-loop corrections to the potential. The discussion on the SM in section 3 follows [4].

Goal: calculate the scalar potential $V(\phi_0, T)$ at finite temperature. The tree-level potential receives quantum corrections. In presence of a heat bath, loop particles can exchange energy-momentum with the bath, and the corrections become temperature dependent.

Work in the grand canonical ensemble: system can exchange energy, charge and particles with the heat reservoir, while temperature, volume and chemical potentials are kept fixed. For simplicity, set the chemical potentials to zero.

The state of the system is described by the density operator ρ . The partition function is defined as the trace over the density operator (units $k_B = 1$)

$$Z = \text{tr}\rho = \text{tr}(e^{-\beta H}) = e^{-\frac{F}{T}}, \quad \beta = 1/T \quad (2.1)$$

which is related to the Helmholtz free energy F as given above. All thermodynamic quantities can be derived from the partition function, e.g. the pressure is $P = T(\partial \ln Z)/(\partial \mathcal{V})$. We are interested in the free energy density, which is minimized in equilibrium, and can be interpreted in a constant background as the effective potential: $V_{\text{eff}} = F/\mathcal{V}$ with \mathcal{V} the volume.

2.1 KMS relation

In a heat bath, the expectation value of an operator should be calculated as the ensemble average with a Boltzmann weight factor $\langle A \rangle = \frac{1}{Z} \text{tr}(A\rho)$. Consider the 2pt correlation function.

$$\begin{aligned} \langle \phi(\mathbf{x}, t)\phi(\mathbf{y}, 0) \rangle &= \frac{1}{Z} \text{tr} \left(e^{-\beta H} \phi(\mathbf{x}, t)\phi(\mathbf{y}, 0) \right) = \frac{1}{Z} \text{tr} \left(e^{-\beta H} \phi(\mathbf{x}, t)e^{-\beta H} e^{\beta H} \phi(\mathbf{y}, 0) \right) \\ &= \frac{1}{Z} \text{tr} \left(\phi(\mathbf{x}, t)e^{-\beta H} e^{i(-i\beta)H} \phi(\mathbf{y}, 0)e^{-i(-i\beta)H} \right) = \frac{1}{Z} \text{tr} \left(\phi(\mathbf{x}, t)e^{-\beta H} \phi(\mathbf{y}, -i\beta) \right) \\ &= \langle \phi(\mathbf{y}, -i\beta)\phi(\mathbf{x}, t) \rangle \end{aligned} \quad (2.2)$$

Here we used the cyclic property of the trace, and the action of an operator under the time-evolution operator

$$U(t) = e^{-iHt}, \quad A(\mathbf{x}, t) = U(t)^\dagger A(\mathbf{x}, 0)U(t). \quad (2.3)$$

We see that $-i\beta$ plays the role of time variable. Define the imaginary time variable

$$\tau = it. \quad (2.4)$$

to write eq. (2.2) in the form

$$\langle \phi(\mathbf{x}, \tau)\phi(\mathbf{y}, 0) \rangle_\beta = \langle \phi(\mathbf{y}, \beta)\phi(\mathbf{x}, \tau) \rangle_\beta \quad (2.5)$$

This is the Kubo-Martin-Schwinger (KMS) relation, which holds for a system in thermal equilibrium.

Lessons from the KMS relation:

Lesson 1: The fields are (anti)-periodic in imaginary time with period β

$$\phi(\mathbf{x}, 0) = \pm\phi(\mathbf{x}, \beta) \quad (2.6)$$

with plus sign for bosons, and minus sign for (the anti-commuting) fermions. One can expand the field in a Fourier series

$$\phi(\mathbf{x}, \tau) = \sum_n \phi(\mathbf{x}, \omega_n) e^{i\omega_n \tau}, \quad \omega_n = \begin{cases} \frac{2\pi n}{\beta}, & \text{bosons,} \\ \frac{2\pi(n+1/2)}{\beta}, & \text{fermions.} \end{cases} \quad (2.7)$$

with Matsubara frequencies ω_n . The finiteness of the time interval makes the energy variable discrete.

Lesson 2: The analogy of the density operator eq. (2.1) with the quantum-mechanical time evolution operator eq. (2.3) underlies the statement that the finite temperature equilibrium field theory is equivalent to the Euclidean theory defined on a finite ‘time’ interval. Many methods developed for the description of zero-temperature quantum field theory can be generalized to the non-zero temperature case.

In QFT the generating function can be expressed in terms of a path integral

$$Z = \int d\phi_i d\phi_f \langle \phi_f(\mathbf{x}, T) | e^{-iHT} | \phi_i(\mathbf{x}, 0) \rangle = \int \mathcal{D}\phi e^{i \int_0^T d^4x \mathcal{L}(\phi)} \quad (2.8)$$

with boundary conditions $\phi(0) = \phi_i$ and $\phi(T) = \phi_f$ (here the wave functions $\langle 0 | \phi_f \rangle \langle \phi_i | 0 \rangle$ are suppressed, as is usually done, as they constitute an irrelevant normalization factor). The path integral runs along the contour \mathcal{C} that spans from $0 < t < T$.

The finite temperature partition function is obtained from this by Wick rotating to euclidean time, and compactifying the Euclidean time direction

$$Z = \text{tr}(\rho) = \int d\phi \langle \phi | e^{-\beta H} | \phi \rangle = \int \mathcal{D}\phi e^{-\int_0^\beta d\tau \int d^3x \mathcal{L}_E} \quad (2.9)$$

with (anti) periodic boundary conditions $\phi(0) = \pm\phi(\beta)$, and with $\mathcal{L}_E = -\mathcal{L}(t \rightarrow \tau = it)$ the Euclidean action. The path integral contour \mathcal{C} now spans from $0 < \tau < \beta$.

2.2 Real scalar field

The goal is to calculate the one-loop potential in field theory at finite temperature. This can be derived from the free (quadratic) Lagrangian, which itself can be viewed as a collection of harmonic oscillators, one for each momentum mode \mathbf{k} . Let's thus start with quantum mechanics and the harmonic oscillator first.

2.2.1 QM at zero temperature

Consider the action

$$S = \frac{1}{2} \int dt [(\partial_t q)^2 - \omega^2 q^2] = -\frac{1}{2} \int d\tau [(\partial_\tau q)^2 + \omega^2 q^2] = -S_E \quad (2.10)$$

with $\tau = it$. The Euclidean version of the generating function is

$$Z = \int dq_f dq_i \langle q_f | e^{-HT} | q_i \rangle = \int [dq] e^{-S_E}, \quad (2.11)$$

We are interested in the energy $E = -\frac{1}{T} \ln Z$ of the system, and we can be cavalier with the normalization factors of Z .

The Hamiltonian for the harmonic oscillator is $H = \omega(N + \frac{1}{2})$, and $H|n\rangle = E_n|n\rangle = \omega(n + \frac{1}{2})|n\rangle$. Using this for the l.h.s. of eq. (2.11) gives

$$Z = \int dq_f dq_i \langle q_f | e^{-HT} | q_i \rangle = \sum_n e^{-E_n T} \int dq_f dq_i \langle q_f | n \rangle \langle n | q_i \rangle, \quad F = \lim_{T \rightarrow \infty} \left(-\frac{1}{T} \ln Z\right) = \frac{1}{2}\omega \quad (2.12)$$

In the limit of euclidean time $T \rightarrow \infty$ the free energy F is dominated by the lowest lying energy state with $n = 0$ and $F = E_0 = \frac{1}{2}\omega$.

Now consider the r.h.s. of eq. (2.11). Let q_n be eigenfunctions of

$$(-\partial_\tau^2 + \omega^2)q_n = \lambda_n q_n, \quad (2.13)$$

The path integral becomes a product of Gaussian integrals and

$$Z = \int [dq] e^{-S_E} = \int dq_n e^{-\frac{1}{2} \int d\tau q_n [-\partial_\tau^2 + \omega^2] q_n} = \det[-\partial_\tau^2 + \omega^2]^{-1/2} \quad (2.14)$$

The determinant can be written as

$$\ln \det[\epsilon^2 + \omega^2] = \ln \prod_n \lambda_n = \sum_n \ln \lambda_n = \text{Tr} \ln(\partial_\tau^2 + \omega^2) = T \int \frac{d\epsilon}{(2\pi)} \ln(\epsilon^2 + \omega^2) \quad (2.15)$$

In the 2nd step we made a fourier transform and took the $T \rightarrow \infty$ continuum limit. From QFT book (e.g. see Peskin & Schroeder eq. 11.73) we find (for d spacetime dimensions)

$$\frac{1}{\mathcal{V}T} \ln Z = \frac{1}{\mathcal{V}T} \ln \det[k_E^2 + \omega^2] = \int \frac{d^d k_E}{(2\pi)^d} \ln[k_E^2 + \omega^2] = -\frac{\Gamma(-d/2)}{(4\pi)^{d/2}} (\omega^2)^{d/2} \quad (2.16)$$

For the one-dimensional QM case $d = 1$ and $\mathcal{V} = 1$, then

$$F = \lim_{T \rightarrow \infty} \left(-\frac{1}{T} \ln Z\right) = -\frac{1}{2} \int \frac{d\epsilon}{(2\pi)} (\epsilon^2 + \omega^2) = \frac{1}{2}\omega \quad (2.17)$$

which agrees with eq. (2.12).

2.2.2 QM at finite temperature

Now consider the harmonic oscillator at finite temperature. The difference with the previous subsection is that now the euclidean time interval $0 \leq \tau \leq \beta$ is compact. The partition function is

$$Z = \int dq \langle q | e^{-H\beta} | q \rangle = \int [dq] e^{-S_E} \quad (2.18)$$

The l.h.s. now becomes

$$Z \sim \sum_n e^{-\beta\omega(n+\frac{1}{2})} \langle n | q \rangle \langle q | n \rangle \sim \frac{e^{-\beta\omega/2}}{1 - e^{-\beta\omega}}, \quad F = \frac{1}{2}\omega + T \ln(1 - e^{-\beta\omega}) \quad (2.19)$$

where we used $F = -T \ln Z$. The first term is the zero temperature contribution, same as we found before eq. (2.12).

Working with the rhs of eq. (2.18), now instead expand q in a fourier series

$$q(\tau) = \sqrt{\beta} \sum_n e^{i\omega_n \tau} \tilde{q}(\omega_n), \quad \text{normalized such that : } \int_0^\beta d\tau e^{i(\omega_n + \omega_m)\tau} = \beta \delta_{m,n}. \quad (2.20)$$

with $\epsilon_n = \omega_n$ the matsubara frequencies. The normalization is chosen such that the Fourier-transformed fields $\tilde{q}(\omega_n)$ are dimensionless. The 2nd expression is the δ -function representation. With this notation the euclidean action becomes

$$\int_\tau \mathcal{L}_E = \beta \sum_{n,m} \int_\tau \frac{1}{2} (\omega_n^2 + \omega^2) \tilde{q}_m \tilde{q}_n e^{i(\omega_n + \omega_m)\tau} = \frac{\beta^2}{2} \sum_n (\omega_n^2 + \omega^2) \tilde{q}_{-n} \tilde{q}_n \quad (2.21)$$

The path integral then becomes a product of Gaussian integrations and

$$Z = \int [dq] e^{-S_E} = \prod_n \int [dq] e^{-\frac{\beta^2}{2} (\omega_n^2 + \omega^2) q_n q_{-n}} \sim \prod_n (\beta^2 (\omega_n^2 + \omega^2))^{-1/2} = \frac{e^{-\beta\omega/2}}{1 - e^{-\beta\omega}}, \quad (2.22)$$

which gives the same result as before eq. (2.19). The sum over matsubara frequencies is left as an exercise.

2.2.3 QFT at finite temperature

Consider a real scalar field with Lagrangian

$$\mathcal{L} = \frac{1}{2} (\partial_\mu \phi)^2 - V(\phi) = -\frac{1}{2} ((\partial_\tau \phi)^2 + (\nabla \phi)^2 + V) = -\mathcal{L}_E \quad (2.23)$$

The partition function is

$$Z = \int d\phi_f d\phi_i \langle \phi_f | e^{-H\beta} | \phi_i \rangle = \int [dq] e^{-S_E} \quad (2.24)$$

In a constant background the effective potential is given by the free energy density eq. (2.1).

Let's expand the field around a classical background

$$\phi(\mathbf{x}, t) = \phi_0 + \varphi(\mathbf{x}, t) \quad (2.25)$$

The lagrangian can be expanded in the number of field fluctuations $\mathcal{L}_E = \mathcal{L}_E^{(0)} + \mathcal{L}_E^{(1)} + \mathcal{L}_E^{(2)} + \dots$. The linear term is proportional to the equations of motion and vanishes on-shell, while

$$\mathcal{L}_E^{(0)} = V_0, \quad \mathcal{L}_E^{(2)} = \frac{1}{2} ((\partial_\tau \varphi)^2 + (\nabla \varphi)^2 + m^2 \varphi^2) \quad (2.26)$$

with classical potential $V_0 \equiv V(\phi_0)$ and with background field dependent mass $m^2 = V''(\phi_0)$. Consider the system in a finite volume \mathcal{V} , with Fourier transform and delta-function normalization

$$\varphi(\mathbf{x}, \tau) = \frac{1}{\sqrt{\mathcal{V}}} \sum_{\mathbf{k}} e^{i\mathbf{k}\cdot\mathbf{x}} \varphi(\mathbf{k}, \tau), \quad \int d^3x e^{i(\mathbf{k}+\mathbf{p})\cdot\mathbf{x}} = \mathcal{V} \delta_{\mathbf{p},\mathbf{k}} \quad (2.27)$$

The quadratic action becomes

$$\mathcal{L}_E^{(2)} = \frac{1}{2} \sum_{\mathbf{k}} (|\partial_\tau \varphi_{\mathbf{k}}|^2 + \omega_{\mathbf{k}}^2 |\varphi_{\mathbf{k}}|^2) \quad (2.28)$$

where we used $\varphi_{-\mathbf{k}} = \varphi_{\mathbf{k}}^*$. This is just k copies of the harmonic oscillator Lagrangian of quantum mechanics with frequency $\omega_{\mathbf{k}} = \sqrt{|\mathbf{k}|^2 + m^2}$. Hence, one can treat the free field as a sum of harmonic oscillators, and re-use the QM results – only need to sum over all k -modes.

Starting with the l.h.s. of the partition function eq. (2.11). The Hamiltonian is $H = \mathcal{V}V_0 + \sum_{\mathbf{k}} \beta \omega_{\mathbf{k}} (N_{\mathbf{k}} + \frac{1}{2})$. Then

$$Z \sim e^{-\beta \mathcal{V} V_0} \sum_{n, \mathbf{k}} e^{-\beta \omega_{\mathbf{k}} (n + \frac{1}{2})} = e^{-\beta \mathcal{V} V_0} \sum_{\mathbf{k}} \frac{e^{-\beta \omega_{\mathbf{k}}/2}}{1 - e^{-\beta \omega_{\mathbf{k}}}}, \quad (2.29)$$

and the effective potential becomes

$$V_{\text{eff}} = \frac{F}{\mathcal{V}} = -\frac{T}{\mathcal{V}} \ln Z = V_0 + \int \frac{d^3\mathbf{k}}{(2\pi)^3} \left(\frac{1}{2} \omega_{\mathbf{k}} + T \ln(1 - e^{-\beta \omega_{\mathbf{k}}}) \right) \quad (2.30)$$

In the last step we took the thermodynamic limit of infinite volume $\sum_{\mathbf{k}} \rightarrow \mathcal{V} \int \frac{d^3\mathbf{k}}{(2\pi)^3}$.

We can also work with the r.h.s. of eq. (2.24).

$$Z = \int \mathcal{D}\phi e^{-\int d\tau d^3x (\mathcal{L}_E^{(0)} + \mathcal{L}_E^{(2)} + \dots)} = e^{-\int d\tau d^3x \mathcal{L}_E^{(0)}} \int \mathcal{D}\phi e^{-\int d\tau d^3x \mathcal{L}_E^{(2)}} \quad (2.31)$$

The zeroth order term gives again the classical potential. The quadratic term is needed for the one-loop contribution.

$$V_{\text{eff}} = -\frac{1}{\beta \mathcal{V}} \ln Z = -\frac{1}{\beta \mathcal{V}} (\ln Z^{(0)} + \ln Z^{(2)}) = V_0 - \frac{1}{\beta \mathcal{V}} \ln \int \mathcal{D}\phi e^{-\int d\tau d^3x \mathcal{L}_E^{(2)}} \quad (2.32)$$

The steps are the same as in the QM case, except that everywhere a summation over momentum is carried along. In particular we Fourier expand the field

$$\varphi(\mathbf{x}, \tau) = \sqrt{\frac{\beta}{\mathcal{V}}} \sum_{\mathbf{k}, n} e^{i(\omega_n \tau + \mathbf{k}\cdot\mathbf{x})} \varphi(\mathbf{k}, \omega_n) \quad (2.33)$$

The normalization is chosen such that the Fourier-transformed fields $\varphi(\mathbf{k}, \omega_n)$ are dimensionless. The partition function becomes

$$Z^{(2)} \sim \prod_{n,\mathbf{k}} \int d\phi_{n,\mathbf{k}} e^{-\frac{\beta^2}{2} \sum_{n,\mathbf{k}} (\omega_n^2 + \omega_{\mathbf{k}}^2) |\varphi_{n,\mathbf{k}}|^2} \sim \prod_{n,\mathbf{k}} (\beta^2 (\omega_n^2 + \omega_{\mathbf{k}}^2))^{-1/2} \quad (2.34)$$

The 1-loop free energy density becomes $V_{\text{eff}} = V_0 + V_{\text{loop}}$ with

$$\begin{aligned} V_{\text{loop}}(\phi_0, T) &= \frac{1}{2\beta\mathcal{V}} \sum_{n,\mathbf{k}} \ln(\beta^2 (\omega_n^2 + \omega_{\mathbf{k}}^2)) = \frac{1}{2\beta\mathcal{V}} \sum_{\mathbf{k}} \left(\beta\omega_{\mathbf{k}} + 2\ln(1 - e^{-\beta\omega_{\mathbf{k}}}) \right) \\ &\stackrel{\nu \rightarrow \infty}{=} \int \frac{d^3\mathbf{k}}{(2\pi)^3} \left(\frac{\omega_{\mathbf{k}}}{2} + \frac{\ln(1 - e^{-\beta\omega_{\mathbf{k}}})}{\beta} \right) \end{aligned} \quad (2.35)$$

where we dropped unimportant constant contributions. The summation over Matsubara frequencies can be done by contour integral, which is left as an exercise. Same result as before eq. (2.30).

The quantum corrections to the potential correspond to the 1-loop vacuum diagrams. They only depend on the effective mass appearing in the propagator, and the results can be extracted from the quadratic potential.

The first term in the brackets in eq. (2.35) is the zero temperature contribution, which sums over the frequencies of all modes – for a free field all the momentum modes are independent harmonic oscillators with zero-point energy $E_{\mathbf{k}} = \frac{1}{2}\omega_{\mathbf{k}}$. This term is divergent, and the divergence can be absorbed in counter terms of the Lagrangian. This term is the one-loop Coleman-Weinberg contribution to the potential. The 2nd term in the brackets is the finite temperature correction to the potential, which we will denote by V_T . Note that the effective mass entering $\omega_{\mathbf{k}}$ is background field dependent $m^2 = V''(\phi_0)$, and both terms contribute to the shape of the potential.

At high temperature $T^2 \gg m^2$ the temperature corrections to the potential are

$$V_T = \int \frac{d^3\mathbf{k}}{(2\pi)^3} \left(\frac{\ln(1 - e^{-\beta\omega_{\mathbf{k}}})}{\beta} \right) = -\frac{\pi^2 T^4}{80} + \frac{\pi^2 m^2 T^2}{24} - \frac{m^3 T}{12\pi} + \dots \quad (2.36)$$

The first term is the free energy of a free boson gas. It is field independent and only shifts the height of the potential, butv does not affect the dynamics of the PT. The 2nd term is a temperature dependent mass term $m^2 T^2 \sim \phi_0^2 T^2$ (where we assumed a mass $m^2 \sim c_i \phi_0^2$), it will dominate at high temperature over the (negative) scalar mass in the tree level potential, and thus the minimum at high T is at the origin. The order of the PT will depend on the $m^3 \sim \phi_0^3$ contribution.

2.3 Breakdown of thermal perturbation theory

At zero temperature the expansion parameters in perturbation theory are the couplings in the theory. From e.g. QCD we know that interactions can be enhanced by the effects of soft/collinear radiation, as the propagators for these particles are large. Similar amplifications

can be seen in the finite temperature theory. The propagators are $\propto \sum_n (\omega_n^2 + \mathbf{k}^2 + m^2)^{-1}$. For light/massless fields, the bosonic Matsubara modes with $n = 0$ and for soft momenta $\mathbf{k}^2 \ll T^2$ give a large enhancement resulting in the breakdown of perturbation theory. To deal with this problem one needs to resum the IR contributions. The leading order effect is that we have to replace the mass of the bosons in the propagators with the temperature corrected mass (which can be extracted from the expansion of J_B): $m^2 \rightarrow m^2 + cT^2$. The IR problems arose because we were expanding around the wrong mass, which is far from the effective mass at finite temperature.

Thus the leading order correction at large temperature from IR effects can be included by replacing the mass with the thermal mass for the bosons (Higgs, Goldstone, and longitudinal modes of the gauge fields) in J_B in V_T in eq. (3.8). Although this improves perturbation theory, close to the phase transition temperature there are still issues. First, the above procedure breaks down for the effective Higgs mass which is $m^2 + cT^2 \sim 0$ for some ϕ . Also the High temperature expansion becomes less good, and higher order (two loops, further IR resummation) need to be included. Another approach is to derive an EFT that only include the light $n = 0$ bosonic modes. This is an active area of research.

2.4 Exercises

2.4.1 Exercise: Equilibrium dynamics

We have assumed that the system is in thermal equilibrium. Show that this is a good approximation for the thermal plasma near the electroweak scale.

- (a) The fastest reactions are those associated with the strong interactions, e.g. $q\bar{q} \rightarrow GG$. A typical weak interaction is $e\nu \rightarrow e\nu$. The slowest interactions involve chirality flips for the lightest fermion, e.g. $e_R H \rightarrow \nu W$. Estimate the interaction rates $\Gamma_{\text{strong}}, \Gamma_{\text{weak}}, \Gamma_{\text{flip}}$ for these interactions.
- (b) Compare the interaction rate with the rate of expansion of the universe at temperature $T \sim 100 \text{ GeV}$ corresponding to the electroweak scale. Is the equilibrium approximation a good approximation?

2.4.2 Exercise: Summation over bosonic Matsubara frequencies

1. Proof the first line of eq. (2.35) where it was used that the sum over Matsubara frequencies in the free energy gives

$$\sum_n \ln(\beta^2(\omega_n^2 + \epsilon_k^2)) = \beta\epsilon_k + 2 \ln(1 - e^{-\beta\epsilon_k}) \quad (2.37)$$

with $\epsilon_k = \omega_{\mathbf{k}}$.

- (a) Verify that

$$T \sum_n \frac{1}{\omega_n^2 + \epsilon_k^2} = -\frac{1}{2\pi i} \oint_{\mathcal{C}} d\omega \frac{1}{\omega_n^2 - \epsilon_k^2} \frac{1}{2} \coth \frac{\omega}{2T} \quad (2.38)$$

with $\omega_n = 2\pi Tn$. Use for this the residue theorem

$$\frac{1}{2\pi i} \oint_{\mathcal{C}} dz f(z) = \sum_n \text{Res} f(z)|_{z=z_n} \quad (2.39)$$

with z_n the poles of $f(z)$ in the area enclosed by the contour \mathcal{C} . For $f(z) = \varphi(z)/\psi(z)$ the residues are

$$\text{Res} f(z)|_{z=z_n} = \frac{\varphi(z_n)}{\psi'(z_n)}. \quad (2.40)$$

(b) Deform the contour to show

$$T \sum_n \frac{1}{\omega_n^2 + \epsilon_k^2} = \frac{1}{2\epsilon_k} \coth \frac{\epsilon_k}{2T} = \frac{1}{2\epsilon_k} (1 + 2f_B(\epsilon_k)) \quad (2.41)$$

with $f_B(\epsilon) = (e^{\epsilon/T} - 1)^{-1}$ the Bose distribution.

(c) Verify that the Matsubara sum can be rewritten as

$$\sum_n \ln(\beta^2(\omega_n^2 + \omega_{\mathbf{k}}^2)) = \sum_n \ln(1 + (\omega_n/T)^2) + \int_1^{(\epsilon_k/T)^2} dx \sum_n \frac{1}{(\omega_n/T)^2 + x^2} \quad (2.42)$$

Now use the result of (b) to proof eq. (2.37).

3 Thermal corrections to the SM Higgs potential and order of the PT

We begin by defining the SM Lagrangian. We write the Lagrangian in terms of left-handed quark and lepton doublets, q_L , and, l_L , respectively, and right-handed singlets u_R , d_R , and e_R . The field H represents the $SU_L(2)$ Higgs doublet of scalar fields H^a . We define $\tilde{H}^a = \epsilon^{ab} H^{b*}$, where ϵ^{ab} is the antisymmetric tensor in two dimensions ($\epsilon^{12} = +1$). The covariant derivative is given by

$$D_\mu = \partial_\mu - i\frac{g_s}{2} G_\mu^a \lambda^a - i\frac{g}{2} W_\mu^i \tau^i - ig' Y B_\mu, \quad (3.1)$$

where g_s , g , and g' are, respectively, the $SU_c(3)$, $SU_L(2)$, and $U_Y(1)$ coupling constants. $\lambda^a/2$ and $\tau^i/2$ denote $SU(3)$ and $SU(2)$ generators, in the representation of the field on which the derivative acts. The hypercharge assignments, Y , are $1/6$, $2/3$, $-1/3$, $-1/2$, -1 , and $1/2$ for q_L , u_R , d_R , l_L , e_R , and H , respectively. The field strengths are

$$G_{\mu\nu}^a = \partial_\mu G_\nu^a - \partial_\nu G_\mu^a - g_s f^{abc} G_\mu^b G_\nu^c, \quad (3.2)$$

$$W_{\mu\nu}^i = \partial_\mu W_\nu^i - \partial_\nu W_\mu^i - g \epsilon^{ijk} W_\mu^j W_\nu^k, \quad (3.3)$$

$$B_{\mu\nu} = \partial_\mu B_\nu - \partial_\nu B_\mu, \quad (3.4)$$

with f^{abc} and ϵ^{ijk} denoting the $SU(3)$ and $SU(2)$ structure constants.

The SM Lagrangian is then written as

$$\begin{aligned} \mathcal{L}_{SM} = & (D_\mu H)^\dagger D^\mu H - \lambda(H^\dagger H - \frac{1}{2}v^2)^2 - \left(\bar{q}_L Y_u \tilde{H} u_R + \bar{q}_L Y_d H d_R + \bar{l}_L Y_e H e_R + \text{h.c.} \right) \\ & - \frac{1}{4} (G_{\mu\nu}^a G^{a\mu\nu} + W_{\mu\nu}^i W^{i\mu\nu} + B_{\mu\nu} B^{\mu\nu}) + \sum \bar{\psi} i \not{D} \psi. \end{aligned} \quad (3.5)$$

where the sum in the last term is over all fermions $\psi = \{q_L, u_R, d_R, l_L, e_R\}$. The terms on the first line are the Higgs kinetic term, the Higgs potential, and the yukawa interactions, whereas the 2nd line gives the kinetic terms for the gauge fields and the fermions. We parameterize the Higgs doublet

$$H = \frac{1}{\sqrt{2}} \begin{pmatrix} \theta_2 + i\theta_3 \\ \phi + h + i\theta_1 \end{pmatrix} \quad (3.6)$$

with ϕ the classical background, and h and θ_i the Higgs and Goldstone boson fluctuations. Expanding around the background $\mathcal{L}^{(0)}$ gives the classical potential

$$V_0 = -\mathcal{L}^{(0)} = \frac{\lambda}{4}(\phi^2 - v^2)^2 = -\frac{1}{2}\mu^2\phi^2 + \frac{\lambda}{4}(\phi^4 + v^4) \quad (3.7)$$

with $\mu^2 = \lambda v^2$. The vacuum Higgs vev is $v = 246 \text{ GeV}$. The vacuum Higgs mass $\partial^2 V|_{\phi=v} = m_\phi^2 = 2\lambda v^2 = (125 \text{ GeV})^2$, from which it follows $\lambda = \frac{1}{2}(m_H/v)^2 \approx 0.12$.

The temperature corrections come from the one-loop diagrams, with all SM particles running in the loop. These loop diagrams are ϕ -dependent, as the masses of the particles will depend on the Higgs field value. The EW gauge bosons and the top quark couple most strongly to the Higgs field, and diagrams with these particles in the loop will dominate the thermal corrections to the potential. The potential at one loop order is $V = V_{\text{tree}} + V_{\text{CW}} + V_T$, with V_{CW} the zero temperature one-loop correction. The thermal potential is

$$V_T = \sum_{\text{boson}} n_i T^4 J_B \left(\frac{m_i^2}{T^2} \right) - \sum_{\text{fermion}} n_i T^4 J_F \left(\frac{m_i^2}{T^2} \right) \quad (3.8)$$

where the sum is over all boson and fermion fields running in the one-loop diagram (all fields that have a ϕ -dependent mass term). Further n_i are the d.o.f. and the thermal functions are given by

$$\begin{aligned} J_B(y^2) &= \frac{1}{2\pi^2} \int_0^\infty dx x^2 \ln(1 - e^{-\sqrt{x^2+y^2}}) \stackrel{y \ll 1}{\approx} -\frac{\pi^2}{90} + \frac{y^2}{24} + \frac{y^3}{12\pi} + \mathcal{O}(y^4), \\ J_F(y^2) &= \frac{1}{2\pi^2} \int_0^\infty dx x^2 \ln(1 + e^{-\sqrt{x^2+y^2}}) \stackrel{y \ll 1}{\approx} \frac{7\pi^2}{720} - \frac{y^2}{48} + \mathcal{O}(y^4). \end{aligned} \quad (3.9)$$

The last expression can be used for the high temperature regime. The scalar contribution to V_T is of the form for a single scalar field derived in the previous section. Now we sum over all bosons in the theory. The fermion contribution has an overall minus sign as a fermion loop gets an overall sign due to the anti-commuting nature of the fields. Note that at high temperature the fermion loop diagrams do not contribute to the cubic correction to the Higgs potential $V \sim \phi^3 T$, which only comes from the boson loops.

For the SM the largest thermal corrections come from the (Higgs, Goldstone), EW gauge fields, and top quark.

$$\Phi = \{h, \theta, W^\pm, Z, t\}, \quad m^2/\phi^2 = \{3\lambda, \lambda, \frac{1}{4}g^2, \frac{1}{4}(g^2 + g'^2), \frac{1}{2}y_t^2\}, \quad n = \{1, 3, 6, 3, 12\} \quad (3.10)$$

Neglecting the CW-potential for simplicity (one can think of the couplings as running couplings due to quantum corrections), the potential at high temperature can be written as

$$V = \frac{1}{2}(-\lambda v^2 + aT^2)\phi^2 - \frac{1}{3}bT\phi^3 + \frac{\lambda}{4}\phi^4 = \frac{1}{2}a(T^2 - \bar{T}^2)\phi^2 - \frac{1}{3}bT\phi^3 + \frac{\lambda}{4}\phi^4 \quad (3.11)$$

with $\bar{T}^2 = (\lambda/a)v^2$ and

$$a = \frac{1}{2}\lambda + \frac{3}{16}(3g^2 + g'^2) + \frac{1}{4}y_t^2, \quad b = \frac{1}{16\pi} \left(12(1 + \sqrt{3})\lambda + 3g^3 + \frac{3}{2}(g^2 + g'^2)^{3/2} \right) \quad (3.12)$$

The couplings measured at the EW scale are $\{\lambda, g, g'\} \approx \{0.38, 0.65, 0.12\}$. At high temperature $T^2 > \lambda v^2/a$ the effective mass term is positive, and the origin is a minimum of the potential. The symmetry is restored. For a 1st order transition the potential needs to develop a barrier between the degenerate minima, for which the cubic correction is essential. The critical temperature for a 1st order PT is defined as the temperature at which the two minima are degenerate. The potential at the critical temperature can then be written in the following form, with degenerate minima at $h = 0$ and $h = v_c$

$$V(T_c) = \frac{\lambda}{4}\phi^2(\phi - v_c)^2 = \frac{\lambda}{4}v_c^2\phi^2 - \frac{\lambda}{2}v_c\phi^3 + \frac{\lambda}{4}\phi^4 \quad (3.13)$$

Note that $v_c \neq v$. Comparing eqs. (3.11) and (3.13) gives

$$\frac{1}{2}\lambda v_c = \frac{1}{3}bT_c \quad \& \quad \frac{1}{4}\lambda v_c^2 = \frac{1}{2}a(T_c^2 - \bar{T}^2) \quad \Rightarrow \quad T_c = \frac{\lambda v_c}{\sqrt{a\lambda - \frac{2}{9}b^2}} \quad (3.14)$$

A strong 1st order PT, that may yield interesting out of equilibrium dynamics, is defined as $v_c/T_c \gtrsim 1$. For the SM this requires

$$\frac{v_c}{T_c} = \frac{2b}{3\lambda} \approx \frac{3g^3}{16\pi\lambda} \gtrsim 1 \quad (3.15)$$

Thus a strong 1st order PT occurs for a Higgs mass

$$m_H^2 = \frac{1}{2}\lambda v^2 \lesssim \frac{3g^3 v^2}{32\pi} = (22 \text{ GeV})^2 \quad (3.16)$$

where we used $v = 246 \text{ GeV}$ and $g = 0.65$. This is much lower than the observed Higgs mass. More careful (lattice) calculations give a larger value for the Higgs mass around 70 GeV to obtain a 1st order PT, although better, still significantly below the observed value.

To get a 1st order PT requires new physics beyond the SM. Additional bosonic fields can enhance the cubic term in the thermal potential, e.g. by adding a singlet (with Z_2 symmetry) or Higgs triplet to the SM. In models with singlets (no Z_2 symmetry) or additional Higgs doublets, the extra Higgs field can also get a vev in the vacuum, and thus affect the tree-level form of the potential.

3.1 Exercises

3.1.1 Exercise: Allowed modifications to the Higgs potential

How well is the Higgs potential constrained by observations, and what modification to obtain a 1st order PT are still allowed?

- (a) Consider the potential for the classical Higgs field of the form

$$V = \frac{1}{2}a\phi^2 - \frac{1}{4}b\phi^4 + \frac{1}{6}c\phi^6 \quad (3.17)$$

Calculate the three extrema of the potential $\phi = 0, \phi_{\pm}$ for ($\phi \geq 0$).

- (b) The minimum $\phi_+ = v$ at finite field value is the symmetry breaking minimum today. Calculate the Higgs mass in this minimum $V_{\phi\phi}|_{\phi=v} = m_h^2$. Solve for a, b in terms of the measured quantities m_h, v and c .
- (c) Calculate the value for c such that $V(\phi_-) = 0$ is degenerate with the minimum at the origin $V(\phi = 0) = 0$. This is a good approximation for the parameters needed for a 1st order PT, as this gives the values where a barrier between the two minima appears – when thermal corrections are included there will then be a barrier between the two minima. Note that the barrier cannot be too high either, otherwise the Higgs field will be stuck in the false vacuum. Show that the cutoff scale $c = 1/\Lambda^2$ needed for a 1st order PT is $\Lambda \sim 700$ GeV. This fixes all parameters in the potential.
- (c) Expand the Higgs potential eq. (3.17) around the minimum $\phi = v + h$ and determine the trilinear coupling

$$\mathcal{L} \supset \lambda_3 h^3 \quad (3.18)$$

- (d) The SM Higgs potential is

$$V_{\text{SM}} = -\frac{1}{2}a_{\text{SM}}\phi^2 + \frac{1}{4}b_{\text{SM}}\phi^4. \quad (3.19)$$

Solve for $a_{\text{SM}}, b_{\text{SM}}$ in terms of the measured quantities m_h, v . Expand the Higgs potential around the minimum $\phi = v + h$ and determine the trilinear coupling λ_3^{SM} . Determine the ratio of the trilinear couplings in the theory with the dim-6 operator eq. (3.17) and the SM Higgs potential eq. (3.19):

$$\kappa = \frac{\lambda_3}{\lambda_3^{\text{SM}}} \quad (3.20)$$

LHC measurements constrain $-1 \lesssim \kappa \lesssim 7$. Is the modified Higgs potential eq. (3.17) still allowed by the data?

3.1.2 Excercise: Higgs-singlet model

Add a real singlet field S to the SM

$$\delta\mathcal{L} = \frac{1}{2}(\partial S)^2 - \kappa^2 |H|^2 S^2 - \frac{1}{2} m_s^2 S^2 - \frac{1}{4} \lambda_s S^4 \quad (3.21)$$

The singlet is odd under a Z_2 symmetry $S \rightarrow -S$, which forbids terms of odd powers of S . The singlet does not alter the tree-level form of the Higgs potential, but it gives an additional contribution to the thermal corrections to the Higgs potential, provided the singlet mass is not much larger than the EW scale. Estimate how large the Higgs-singlet coupling κ has to be for a 1st order PT.

4 Tunneling and bubble nucleation

The time evolution operator of quantum mechanics is $U(t) = e^{-iHt}$. If the energy, the eigenvalue of the Hamiltonian, has an imaginary part $\Gamma \sim \text{Im}(E) \neq 0$, the state will decay. We aim to calculate the decay rate for the false vacuum via bubble nucleation during a first order PT.

Useful reference for phase transitions [5, 6]; the generalization to finite temperature is found in [7].

4.1 QM at zero temperature

Start again with QM, and work with Euclidean time. Consider the Euclidean action

$$S_E = \int d\tau \left[\frac{1}{2} (\partial_\tau q)^2 + V \right] \quad (4.1)$$

The potential with (false) vacuum at $q = q_-$ and true vacuum at $q = q_+$. The equations of motion are

$$\frac{\delta S_E}{\delta q} = -\partial_\tau^2 q + V' = 0, \quad \Rightarrow \quad \partial_\tau \left(\frac{1}{2} (\partial_\tau q)^2 - V \right) = 0 \quad (4.2)$$

These are the equations of motion for a particle moving in a potential $-V$, and $E = \frac{1}{2} (\partial_\tau q)^2 - V$ is a constant of motion. We have already considered the trivial solution $q = q_-$ in the previous section. Normalizing $V(q_-) = 0$ the partition function (for $T \rightarrow \infty$) is eq. (2.12)

$$Z = N e^{-FT} = \int [dq] e^{-S_E^{(2)}} = \det[-\partial_\tau^2 + V'']^{-1/2} \sim e^{-\frac{1}{2}\omega T} \quad (4.3)$$

with $\omega^2 = V''(q_-)$. As we have seen, this gives the perturbative correction to the effective potential from the fluctuations, and shift the free energy by zero-point fluctuations $F = E_0 = \frac{1}{2}\omega$.

But with also a local minimum of the potential, there is another solution to the equations of motions with finite energy. For the energy to be finite $q(\pm T/2) = q_-$ (remember, the energy for the field at rest is $E = -V$), but at intermediate times the field can go to escape

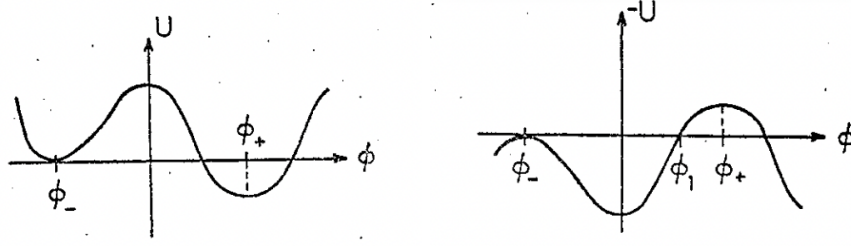


Figure 3. Left: Potential V with false and true vacuum. Right: inverse potential $-V$. From [6];

point σ and back (with σ the point for which $V(\sigma) = 0$). This is the bounce solution, which is the solution to the eom with boundary conditions

$$\partial_\tau q|_{\tau_c} = 0, \quad \lim_{\tau \rightarrow \pm\infty} q = q_- \quad (4.4)$$

with t_c the center of the bounce at field value $q(t_c) = \sigma$, and $q = q_-$ asymptotically. Integrate the eom eq. (4.2) to give

$$\partial_\tau \left(\frac{1}{2} (\partial_\tau q)^2 - V \right) = 0 \quad \Rightarrow \quad \frac{1}{2} (\partial_\tau q)^2 - V = -V(q_-) = 0 \quad \Rightarrow \quad \tau = \int_q^\sigma \frac{dq}{\sqrt{2V}} \quad (4.5)$$

The action for the bounce q_b is

$$B \equiv S_E(q_b) = \int d\tau V = \int_0^\sigma dq \sqrt{2V} \quad (4.6)$$

where we used the eom twice to set $\partial_\tau^2 q = V$ and $(\partial_\tau q) = \sqrt{2V}$. There can be many bounces in the time-interval T . Summing over them gives

$$\begin{aligned} Z &\sim e^{-\frac{1}{2}\omega T} \sum_n \int_{-T/2}^{T/2} d\tau_1 \int_{-T/2}^{\tau_1} d\tau_2 \dots \int_{-T/2}^{\tau_{n-1}} d\tau_n (K e^{-B})^n = e^{-\frac{1}{2}\omega T} \sum_n \frac{(T K e^{-B})^n}{n!} \\ &= e^{-(\frac{1}{2}\omega - K e^{-B})T} \end{aligned} \quad (4.7)$$

K is the determinant from the gaussian perturbations around the bounce solution. As the bounce is not the minimum of the action but a saddle point, the eigenfunction equation has a negative eigenvalue, and $\text{Im}(K) \neq 0$. Now defining the decay probability per unit time by

$$\Gamma = -2\text{Im}E = \frac{2}{T} \text{Im} \ln Z = 2\text{Im}(K) e^{-B} = A e^{-B} = \left(\frac{B}{2\pi} \right)^{1/2} \left| \frac{\det' [-\partial_\tau^2 + V''(q_b)]}{\det [-\partial_\tau^2 + \omega^2]} \right|^{-1/2} e^{-B} \quad (4.8)$$

The action for a single bounce B in eq. (4.6) gives the timescale of decay. Here \det' implies that the zero eigenvalue of the operator $\partial_\tau^2 + V''(q_b)$ is to be omitted. This zero mode corresponds to the time-translational invariance of the bounce solution. We have already included this when integrating over the time translations of the bounce eq. (4.7). The factor $(\frac{B}{2\pi})^{1/2}$ comes from the change of variables in the integration of bounce positions to integration of the time of the bounce. The determinant is hard to compute in practice, but the coefficient A can be estimated from dimensional analysis.

4.2 QFT

Results carry over to QFT. Consider a real scalar with Euclidean action

$$S_E = \int d^4x \left(\frac{1}{2}(\partial_\tau \phi)^2 + \frac{1}{2}(\nabla \phi)^2 + V \right) \quad (4.9)$$

where the potential has a (false) true vacuum at $(\phi = \phi_-)$ $\phi = \phi_+$, and we set $V(\phi_-) = 0$. The Euclidean Lagrangian is invariant under a four- dimensional Euclidean rotation. The lowest energy bounce solutions is $O(4)$ symmetric. Define $\rho = \sqrt{r^2 + \tau^2}$. The bounce then solves the eom with boundary conditions

$$\square \phi = \partial_\rho^2 \phi + \frac{3}{\rho} \partial_\rho \phi = \partial_\phi V \quad (4.10)$$

$$\lim_{\rho \rightarrow \infty} \phi = \phi_-, \quad \partial_\rho \phi|_{\rho=0} = 0 \quad (4.11)$$

The equation of motion has a mechanical interpretation (with ρ as time) of a particle moving in a potential $-V$, subject to a a damping force (the first derivative term). The particle is released at rest at time zero. If the initial position is chosen properly, this can be done by adjusting the center of the bounce $\phi_b(\rho = 0) = \phi_0$ using a undershoot/overshoot method, the particle will come to rest at infinite time at ϕ_- , and the solution has finite energy.

The decay rate per unit volume per unit time is $\frac{\Gamma}{\mathcal{V}} = Ae^{-B}$ with

$$B = S_E(\phi_b) - S_E(\phi_-) = (2\pi^2) \int d\rho \left[\frac{1}{2}(\partial_\rho \phi_b)^2 + V(\phi_b) \right] - V(\phi_-),$$

$$A = \left(\frac{B}{2\pi} \right)^2 \left| \frac{\det' [-\partial_\tau^2 + V''(\phi_b)]}{\det [-\partial_\tau^2 + V''(\phi_-)]} \right|^{-1/2} \quad (4.12)$$

with ϕ_b the bounce solution. $S_E(\phi_-)$ is the action for the trivial solution in the false vacuum, which vanishes with our normalization $V(\phi_-) = 0$. There are now 4 zero modes corresponding to translation of the solution along any of the 4 axes in euclidean space.

4.3 Bubble nucleation at finite temperature

At zero temperature the bubbles nucleate because of quantum fluctuations. For $T \neq 0$ thermal fluctuations will also play a role. The dynamics of bubble formation is influenced by temperature.

To include finite temperature one needs to compactify the imaginary time direction $0 < \tau < \beta$. Consider the infinite time axis, where the theory is periodic with period β . For bubble sizes $R \ll \beta$, i.e. $T < R^{-1}$, the bubble is much smaller than the size of the compactified direction, and the finite temperature effects are small. The solution is a series of the $O(4)$ -symmetric bubbles placed at a distance β from each other. As T increases the bubbles become placed closer together, until at $T \sim R^{-1}$ they become overlapping in the time direction. For $T \gg R^{-1}$ the solution is a cylinder, whose spatial cross section is the the $O(3)$ symmetric bubble of some new radius. In other words, the bubble solution can be approximated as

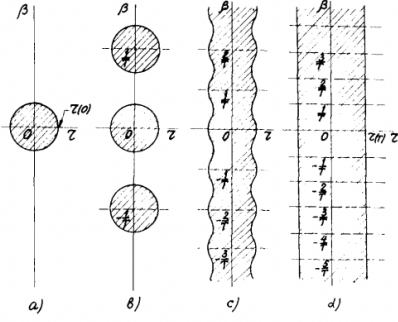


Figure 4. Solution of the bounce equations at different values of the temperature. (a) $T = 0$; (b) $T \ll R^{-1}$; (c) $T \sim R^{-1}$; (d) $T \gg R^{-1}$. The dashed regions contain the classical field $\phi \neq 0$. For simplicity we have shown the bubbles for the case when their wall thickness is less than the bubble radius. From [7].

constant in the time direction, which can be integrated over, and is the solution of the equations of motion in 3 dimensions.

We can then write the euclidean action as

$$B = \int d\tau \int d^3\mathbf{r} \mathcal{L}_E = \beta S_3, \quad S_3 = \int d^3\mathbf{r} \left(\frac{1}{2}(\nabla\phi)^2 + V(\phi, T) \right) \quad (4.13)$$

where we again set $V(\phi_-) = 0$. The bubble will now be $O(3)$ symmetric, and the eom become

$$\square\phi = \partial_\rho^2\phi + \frac{2}{\rho}\partial_\rho\phi = \partial_\phi V \quad (4.14)$$

$$\lim_{\rho \rightarrow \infty} \phi = \phi_-, \quad \partial_\rho\phi|_{\rho=0} = 0 \quad (4.15)$$

with now $\rho = \sqrt{\mathbf{r}^2}$. The different coefficient of the damping term comes from the $\square\phi$ operator in 3 dimensions. The tunneling rate per unit volume is

$$\frac{\Gamma}{\mathcal{V}} = A e^{-S_3/T} = \left(\frac{S_3}{2\pi T} \right)^{3/2} \left| \frac{\det' [\partial_\tau^2 + V''(\phi_b)]}{\det [\partial_\tau^2 + V''(\phi_+)]} \right|^{-1/2} e^{-S_3/T} \quad (4.16)$$

The coefficient $A \sim T^4 \left(\frac{S_3}{2\pi T} \right)^{3/2}$ on dimensional grounds. This gives us an expression for the tunneling rate per unit volume for a given temperature.

4.3.1 Nucleation temperature

The phase transition occurs if the bubbles expand and coalesce, and the whole of space thus transitions to the true vacuum state. For this to happen, at least one bubble per Hubble volume per Hubble time needs to be nucleated. In other words, when $\Gamma \sim H$ – where we used that $\mathcal{V} \sim H^{-3}$ is equal to the Hubble volume – the phase transition takes place. The temperature at which this happens is called the nucleation temperature T_N , which is lower than the critical temperature. For strong phase transitions, happening for potentials with a

large barrier, the phase transition can be delayed with nucleation temperature much smaller than the critical temperature; if the barrier is really large, the universe may be stuck in the false vacuum (on timescales of the age of the universe) and the phase transition never takes place. In the opposite limit, for shallow barriers, one expects $T_N \sim T_c$ to be close.

Using that $H^2 \sim T^4/M_{\text{P}}^2$ during radiation domination, one can estimate the nucleation temperature via

$$\frac{S_3}{T} \sim \ln(H^4/T^4) \sim \ln(M_{\text{P}}^4/T^4) \quad (4.17)$$

For the EW scale $T \sim 10^2$ GeV this gives $S_3/T_N \sim 150$.

4.3.2 Thin wall approximation

Consider the limit that the energy-density difference between the true and false vacuum is much smaller than the height of the barrier. We parameterize the potential

$$\epsilon = V(\phi_-) - V(\phi_+), \quad V = V_0 + \epsilon \frac{(\phi - \phi_-)}{(\phi_+ - \phi_-)} \quad (4.18)$$

with $V_0(\phi_+) = V_0(\phi_-) = 0$ the symmetric part of the potential.

The bounce action S_3 consists of the surface energy of the bubble proportional to $(\nabla\phi)^2$, which is the transition region in which the field changes from the false vacuum outside the bubble to (close to) the true vacuum inside. The surface term scales as $\propto R^2$ and costs energy. The other term is the volume region inside the bubble $V(\phi_+) - V(\phi_-) = -\epsilon$ for $\rho < R$. This contribution scales as $\propto -\epsilon R^3$ and gains energy. It is energetically favorable for the bubble to expand if the volume term wins. For small ϵ this happens only for a large radius R . When the size of the bubble becomes much larger than the thickness of the wall the bounce solution $\phi(\rho)$ stays close to the escape point at $\rho = 0$ for a long time, until at $\rho \sim R$ it rolls to the asymptotic false vacuum solution at $\phi_-(\rho \rightarrow \infty)$. The thin wall approximation consists of dropping the damping term in the eom. At small ρ it is negligible because the field is approximately frozen, whereas when it starts to roll at large radius $\rho \sim R$ the damping term is $1/R$ suppressed.

Dropping the friction term and the ϵ -correction to the potential in the eom eq. (4.14) gives $\phi'' = \partial_\phi V_0$. We have already solved this in the QM example eq. (4.5). Copying that solution gives

$$\rho - \bar{\rho} = \int_{\frac{1}{2}(\phi_- + \phi_+)}^{\phi} \frac{d\phi}{\sqrt{2V_0}} \quad (4.19)$$

with $\bar{\rho}$ the integration constant defined as the coordinate when $\phi(\rho)$ is the average of the two minima.

If $\bar{\rho}$ is large, the bounce looks like a ball of true vacuum, $\phi = \phi_+$, embedded in a sea of false vacuum, $\phi = \phi_-$, with a transition region (“the wall”) separating the two. The wall is small in thickness compared to the radius of the ball $\bar{\rho}$. We can divide the solution in three regions: $\phi = \phi_-$ in the outside region $\rho > \bar{\rho}$, $\phi = \phi_+$ in the inside region $\rho < \bar{\rho}$, and the wall

region $\rho \sim \bar{\rho}$ where the transition takes place. The euclidean action is

$$\begin{aligned}
(S_3)_{\text{outside}} &= 0, \\
(S_3)_{\text{inside}} &= -\frac{4}{3}\pi\bar{\rho}^3\epsilon, \\
(S_3)_{\text{wall}} &\approx 4\pi\bar{\rho}^2 \int d\rho (2V_0) = 4\pi\bar{\rho}^2 \int_{\phi_+}^{\phi_-} d\phi \sqrt{2V_0} \equiv 4\pi\bar{\rho}^3 S_1
\end{aligned} \tag{4.20}$$

where we assumed the wall thickness much smaller than $\bar{\rho}$. S_1 is the action for the 1-dim theory, which gives the surface tension of the bubble. To find the radius R , minimize the action with respect to $\bar{\rho}$

$$\partial_{\bar{\rho}} S_3 \Big|_{\bar{\rho}=R} = \partial_{\bar{\rho}} \left(-\frac{4}{3}\pi\bar{\rho}^3\epsilon + 4\pi\bar{\rho}^2 S_1 \right) \Big|_{\bar{\rho}=R} \Rightarrow R = \frac{2S_1}{\epsilon} \tag{4.21}$$

which gives

$$S_3 = \frac{16\pi S_1^3}{3\epsilon^2} \tag{4.22}$$

as the final result.

4.3.3 Thick wall approximation

If the depth of the minimum $V(\phi_+)$ is sufficiently large, the escape point $\phi_0 = \phi(\rho = 0)$ will be usually far from the minimum $\phi_0 \ll \phi_+$. The field inside the bubble does not reach the true vacuum, and the bubble has a thick wall in which the field value changes. As the bounce solution is not sensitive to the details of the potential close to the true vacuum, it can be a good approximation to Taylor expand the potential, which (depending on the model) often becomes of the form

$$V_1 = \frac{1}{2}m^2\phi^2 - \frac{1}{4}\lambda\phi^4 \quad \text{or} \quad V_2 = \frac{1}{2}m^2\phi^2 - \frac{1}{3}A\phi^3 \tag{4.23}$$

Here we will focus on the potential with the cubic interaction. Rescaling the coordinate $\bar{\rho} = \rho/m$ and rescaling the field $\phi = 3m^2/(2A)\chi$ the potential and equations of motion become

$$V = \frac{1}{2}\chi^2(1 - \chi), \quad \partial_{\bar{\rho}}^2\chi + \frac{2}{\bar{\rho}}\partial_{\bar{\rho}}\chi = \chi - \frac{3}{2}\chi^2 \tag{4.24}$$

where we have chosen the transformation such that the potential vanishes $V(\chi = 1) = 0$ at field value $\chi = 1$. No analytic solution exists, but this equation can easily be solved numerically. The bounce solution and decay rate for arbitrary parameters can then be found by rescaling to the original variables. Explicitly, the finite temperature actions are

$$S_3(\phi) = \frac{9m^3}{4A^2} S_3(\chi) \tag{4.25}$$

with numerically $S_3(\chi) \approx 19.4$ the euclidean bounce for the solutions of eq. (4.24).

4.4 Fate of the false vacuum

Consider first the $T = 0$ case. The classical field makes a quantum jump (say at $t = 0$) to the state defined by

$$\phi(t = 0, \mathbf{x}) = \phi(\tau, \mathbf{x}) \quad (4.26)$$

This implies that the same function, $\phi(\rho)$, that gives the shape of the bounce in four dimensional Euclidean space also gives the shape of the bubble at the moment of its materialization in three-space. At finite t we can analytically continue back to Minkowski space to find

$$\phi(t, \mathbf{x}) = \phi(\rho = \sqrt{|\mathbf{x}|^2 - t^2}) \quad (4.27)$$

The bubble will expand (or collapse), with velocity that soon after its existence will reach the speed of light. The energy is the sum of the negative volume energy term and a positive surface term. For the thin wall solution

$$E = -\frac{4\pi}{3}\epsilon R^3 + 4\pi S_1 R^2 = \frac{4\pi}{3}\rho^2(R_0 - R)\epsilon \quad (4.28)$$

with R_0 the radius of the thin wall bubble at creation. The energy vanishes at bubble creation, dictated by energy conservation, as the energy vanished before the bubble was created. The bubble will expand if the volume term wins and $\partial_R E \geq 0$. The critical bubble where this equation is saturated has $R_c = 2S_1/\epsilon$. Since $R_0 > R_c$ the thin wall bubble will expand.

For the thin wall solution the bubble has a thin wall at $R = R_0$. As the bubble expands, this wall traces out the hyperboloid $|\mathbf{x}|^2 - t^2 = R_0^2$, and the ball expansion soon reaches the speed of light.

At finite temperature the ball will not expand in vacuum but in a thermal plasma. Plasma particles will scatter off and enter the bubble, and as they are massless outside and massive inside, this will take away energy, slowing the bubble down. To calculate the bubble expansion velocity is a very active area of research, as this parameter enters the predictions for baryogenesis and the gravitational wave signal.

4.5 Exercises

4.5.1 Exercise: thin wall solution

The Higgs potential at finite temperature eq. (3.11) is

$$V = \frac{1}{2}a(T^2 - \bar{T}^2)\phi^2 - \frac{1}{3}bT\phi^3 + \frac{\lambda}{4}\phi^4 \quad (4.29)$$

with $\bar{T}^2 = (\lambda/a)v^2$. Assume b receives additional corrections from beyond the SM scalars and a 1st order PT is possible. In eq. (3.14) it was shown that

$$T_c^2(1 - 2b^2/(9a\lambda)) = \bar{T}^2, \quad v_c = \frac{2bT_c}{3\lambda} \quad (4.30)$$

For estimates use $a \sim 0.4$, $b \sim 0.2$, $\lambda \sim 0.1$ and $\bar{T} \sim 130$ GeV. The equation above then gives $T_c \sim 1.1\bar{T} \equiv c\bar{T}$. This gives $v_c/T_c = 2b/(3\lambda) = 1.3$ and allows for a strong PT.

- [a] Express the difference between the false and true vacuum $\epsilon = V(0) - V(v_c)$ as a function of $T_c - T$ in the limit $x \equiv (T - T_c)/\bar{T} \ll 1$.
- [b] In the thin wall limit $x \ll 1$, calculate the surface tension S_1 , the bounce action S_3 and the bubble wall radius R in the thin wall approximation.
- [c] Estimate the bubble wall thickness using

$$\Delta R^{-1} \sim \frac{1}{\phi} \frac{\partial \phi}{\partial \rho} \Big|_{\phi=\frac{1}{2}v_c} \quad (4.31)$$

and find the bound on x for the thin wall approximation $\Delta R \ll R$ to be valid.

- [d] Find the value of x at the nucleation temperature T_n that the phase transition proceeds (approximate $T_n \approx T_c$ in the thin wall limit). Does the phase transition take place in the thin wall regime?

4.5.2 Exercise: thick wall regime

Consider the thick wall regime where the minimum $V(\phi_+)$ is very deep, and the escape point $\phi_0 = \phi(\rho = 0)$ is far from the minimum $\phi_0 \ll \phi_+$. Consider the case that the Taylor expanded potential is of the form

$$V = \frac{1}{2}m^2\phi^2 - \frac{1}{4}\lambda\phi^4 \quad (4.32)$$

- [a] Rescale the field to find the potential and bounce equation in terms of the dimensionless fields only (fix the coefficients by setting $V = 0$ for the rescaled field $\chi = 1$).
- [b] Find the scaling of the bounce with the parameters of the theory, i.e. find $S_3(\phi_3)$ in terms of the bounce for the dimensionless field $S_3(\chi)$.

5 Electroweak baryogenesis

Useful references [4, 8, 9].

The SM interactions are the same for particles and antiparticles, except for the small CP violating phase in the CKM matrix. Yet, everything we see around us is made of matter. The asymmetry between matter and antimatter, or between baryons and anti-baryons, is characterized by the ratio of densities of baryon number and entropy ($s = \frac{2\pi}{45}g_*sT^3$); this ratio has been determined by two independent methods

$$Y_b = \frac{n_b - n_{\bar{b}}}{s} = \frac{1}{7.04} \frac{n_b - n_{\bar{b}}}{n_\gamma} = \begin{cases} 8.2 - 9.4 \times 10^{-11} & \text{BBN} \\ 8.65 \pm 0.09 \times 10^{-11} & \text{CMB} \end{cases} \quad (5.1)$$

with $n_{\bar{b}} \approx 0$. For every 10^{10} photons in the universe there is one baryon.

Big bang nucleosynthesis (BBN) is the period where the light elements, such as deuterium, helium and lithium, are formed. The primordial abundances of these elements, which can be

observed in today's universe, depend sensitively on the ratio of baryons to photons at BBN. The amount of baryons can be extracted from cosmic microwave background measurements as follows. Over densities grow under the action of gravity, and eventually collapse. The collapse is reverted by the photon pressure of the plasma, and this leads to the acoustic oscillations observed in the CMB spectrum. The baryons provide the mass for the collapsing and expanding matter, whereas the photons provide the pressure, and the amount of baryons thus influence the height of the acoustic peaks.

There are many baryogenesis scenarios that provide a dynamical origin for the baryon asymmetry on the market: GUT baryogenesis, baryogenesis from primordial black holes, Affleck-Dine (AD) baryogenesis, baryogenesis at preheating, baryogenesis via leptogenesis, spontaneous baryogenesis, gravitational baryogenesis, defect mediated baryogenesis, B-ball baryogenesis, baryogenesis from CPT breaking, baryogenesis through quantum gravity, axiogenesis, baryogenesis by brane collision, mesogenesis, electroweak baryogenesis, etc. And many of these are a collective name for many different implementations. Unfortunately, many of the scenarios take place at very high energies and will be very hard or even impossible to test with experiment, at least in the foreseeable future. This is not the case for EW baryogenesis, which requires new physics at the EW scale, and thus can be probed by colliders, precision EDM experiments and, in the future, gravitational wave observations.

5.1 Sakharov conditions and EW baryogenesis

Sakharov was the first to realize the need for a baryogenesis mechanism, and in his paper from 1967 – his paper was not cited until 1979 – contains three necessary conditions for any baryogenesis scenario.

1. Baryon number violation. If all reactions/processes have as many baryons in the initial as in the final state, no asymmetry will be created.
2. C and CP violation. C violation is needed, else the rate for particle creation is the same as that for antiparticle creation. CP violation is needed, else the rate for left-chiral particle creation is the same as that for right-chiral antiparticles.¹
3. Departure from thermal equilibrium. If all the particles in the Universe remained in thermal equilibrium, then no preferred direction for time can be defined. All rates are equal to their inverse rates.

Let's see how these conditions are violated in EW baryogenesis. The out of equilibrium dynamics is provided by a first order PT. As we have seen, this requires new physics beyond the SM, otherwise the transition is a cross over, and the physics is close to equilibrium at all times. C is maximally violated by the weak interactions, under which only the left-handed particles are charged. CP is also violated by the phase in the CKM matrix. From the Jarlskog

¹The notation is that \bar{q}_R is the antiparticle of q_R which is left-handed. The subscripts L, R keep track whether the fields transform as a doublet or singlet under $SU(2)$.

invariant one may estimate the size of the CP violation at the EW scale $\delta_{\text{CP}} \sim 10^{-20}$, way too small to create the observed asymmetry. Hence, sufficient CP violation also requires new physics, and for it to be important during the EW PT, this new physics should not be much larger than the TeV scale. As an example, consider the correction to the top quark yukawa interaction

$$\mathcal{L} \supset \frac{y_t}{\sqrt{2}} \phi \left(1 + c \frac{\phi^2}{\Lambda^2} \right) \bar{t}_L t_R + \text{h.c.} \quad (5.2)$$

with ϕ the radial higgs field. The dimension-6 operator can be thought of as generated from integrating new physics at the scale Λ . If $\text{Im}(c) \neq 0$ then CP is violated. In the vacuum $\phi = v + h$, and the effective top mass is $m_t = \frac{y_t}{\sqrt{2}} v \left(1 + c \frac{v^2}{\Lambda^2} \right)$. The phase can be rotated away by a chiral transformation $t_L \rightarrow e^{i\alpha} t_L$ and $t_R \rightarrow e^{-i\alpha} t_R$. This is the standard procedure to make the mass matrix real. (For three generations, there is then one phase that cannot be eliminated, which is the CKM phase.) However, in the CP violating bubble wall background the higgs field value $v(x)$ is space-time dependent, and cannot be rotated away by a global rotation. Hence the effective top mass in the bubble wall background is complex – in particular, inside the bubble wall where the vev changes – and the corresponding CP violation is physical and can generate an asymmetry between t_L and \bar{t}_L .

The CP violating correction to the top-higgs coupling $\bar{t}_L t_R h$ can be probed in EDM experiments, see section 5.3.

Finally, baryon number is violated in the SM by the so-called sphaleron processes.

5.1.1 Sphalerons

Baryon and lepton number are symmetries of the classical action, but they are violated by quantum effects. The current conservation is non-zero for the baryon current $J_B^\mu = \sum_q \frac{1}{3} \bar{q} \gamma^\mu q$ and lepton current $J_L^\mu = \sum_l (\bar{l} \gamma^\mu l + \bar{\nu}_l \gamma^\mu \nu_l)$ because of the anomalous triangle diagrams. Forgetting for simplicity hypercharge and only including the $SU(2)$ symmetry, we can write

$$\partial_\mu J_B^\mu = \partial_\mu J_L^\mu = N_f \frac{g^2}{32\pi^2} F_{\mu\nu} \tilde{F}^{\mu\nu} = N_f \partial_\mu K^\mu, \quad K^\mu = \frac{g^2}{32\pi^2} \epsilon^{\mu\nu\rho\sigma} \left(\partial_\nu A_\rho^a A_\sigma^a - \frac{1}{3} g \epsilon_{abc} A_\nu^a A_\rho^b A_\sigma^c \right) \quad (5.3)$$

with N_f the number of families. $B - L$ is still a good quantum number, but $B + L$ is violated.

Although this is a total derivative, the boundary term does not vanish because of its topological nature. The variation of the total baryon number $B = \int d^3x J_B^0$ is

$$N_f \Delta N_{\text{CS}} = N_f \int d^4x \partial_\mu K^\mu = N_f \int d^4x (\partial_0 K^0 - \partial_i K^i) = N_f \int d^3x K^0|_{t_i}^{t_f} = N_f \Delta B \quad (5.4)$$

In the 3rd expression we dropped the divergence of the spatial current, which by Gauss theorem is equivalent to a surface integral of the flux through it; it is possible to choose a gauge in which this vanishes. The Chern-Simons number N_{CS} is an integer.

The most generic 2×2 unitary matrix with determinant equal to unity may be expressed as $a \mathbb{1} + ib_i \sigma^i$ with the condition $a^2 + |b|^2 = 1$. Therefore the topology of $SU(2) \sim S^3$.

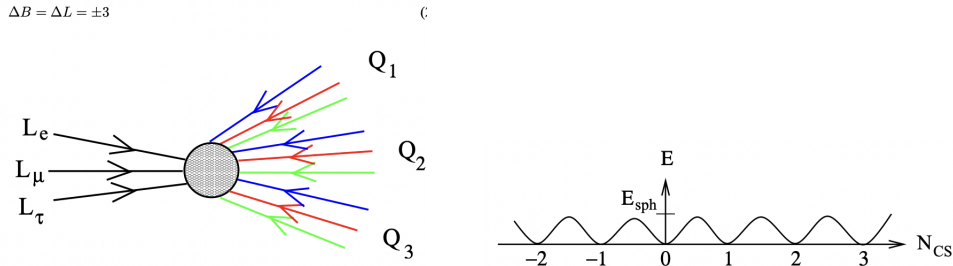


Figure 5. Sphalerons. Left: Feynman diagram for effective sphaleron interaction. Right: Energy of gauge field configurations as a function of Chern-Simons number. Form [4].

Classically, the ground state must correspond to a time-independent field configuration with vanishing energy density $F_{\mu\nu} = 0$, which means that the gauge field is a pure gauge. Let's work in temporal gauge which sets $A_0 = 0$. The temporal gauge is a partial gauge fixing condition, as time-independent gauge transformations $U(\mathbf{x})$ leave the gauge fixing condition $A_0 = 0$ fixed: $A_0 \rightarrow \frac{i}{g}U(\mathbf{x})\partial_0 U^{-1}(\mathbf{x}) = 0$. The vacuum is thus described by the time-independent pure gauge configuration $A(\mathbf{x}) = (i/g)U(\mathbf{x})\nabla U(\mathbf{x})^{-1}$.

We can make use of the remaining gauge freedom to impose at spatial infinity $|\mathbf{x}| \rightarrow \infty$ that $A_i = 0$ by choosing $U = 1$. Spatial infinity with infinity identified is equivalent to S^3 . Hence, by imposing this last condition the gauge transformation $U(\mathbf{x})$ becomes a mapping from S^3 to the gauge group $SU(2) \sim S^3$. These mappings fall into homotopy classes categorized by integer winding numbers. Two mappings $\mathbf{x} \rightarrow U_1(\mathbf{x})$ and $\mathbf{x} \rightarrow U_2(\mathbf{x})$ belong to the same class if there exists a continuous transformation from $U_1(\mathbf{x})$ to $U_2(\mathbf{x})$, which correspond to small gauge transformations, ie gauge transformations that can be continuously deformed to the identity transformation. Mappings in different homotopy classes correspond to distinct vacua, which are related by a large gauge transformation. The energy density vanishes in the different vacua, but to transition costs a finite energy density. The general configuration of the different vacua is given by (up to small gauge transformations)

$$U(\mathbf{x}) = \exp\left(\frac{i\pi\mathbf{x} \cdot \boldsymbol{\sigma}}{\sqrt{|\mathbf{x}|^2 + \lambda^2}}n\right) \quad (5.5)$$

with $n = N_{cs}$ the winding number, and λ an arbitrary scale parameter.

To find the height of the barrier between inequivalent vacua, one can construct the explicit solution that interpolates between the vacuum and the top of the barrier. This is the sphaleron solution, which is Greek for 'ready to fall', as the top of the barrier is an unstable state. The energy of the sphaleron is found to be

$$E_{sph} = f(\lambda/g)\frac{4\pi v}{g}, \quad f(\lambda/g) \sim 2. \quad (5.6)$$

with $v(T)$ the temperature dependent vev in the minimum. For tunneling at finite tempera-

ture the sphaleron transition rate, the barrier crossing rate, is

$$\frac{\Gamma_{\text{sph}}}{V} \sim \begin{cases} e^{-E_{\text{sph}}/T}, & T \lesssim m_W \\ 10^{-6}T^4, & T \gtrsim m_W \end{cases} \quad (5.7)$$

where the constant of proportionality is found from lattice calculations. At high temperature $T \gtrsim m_W$ there is no barrier, as the Higgs field is still in the false vacuum and $E_{\text{sph}} = 0$. The sphaleron effective interactions violates baryon and lepton number by $\Delta B = \Delta L = \pm 3$, and involves quarks (with all colors) and leptons from all generations, see ???. An example $\Delta B = \Delta L = -3$ transition is $u + d \rightarrow \bar{d} + 2\bar{s} + \bar{c} + 2\bar{b} + \bar{t} + \bar{\nu}_e + \bar{\nu}_\mu + \bar{\nu}_\tau$.

At zero temperature the transition can only go via quantum mechanical tunneling, and the bounce solution is proportional to g^{-2} , and the rate is exceedingly small

$$\frac{\Gamma}{V} \sim e^{-8\pi^2/g^2} \sim 10^{-185} \quad (5.8)$$

assuring stability of the proton. At finite temperature the thermal fluctuations may get the fields on top of the barrier, and it can then roll to the next vacuum.

5.2 EW baryogenesis

At high temperature the EW sphalerons are in thermal equilibrium and any preexisting $B-L$ symmetry is washed out. In EW baryogenesis baryon number is generated at the electroweak phase transition. The picture is as follows:

The PT is first order and bubbles of true vacuum are nucleated, and expand into the surrounding plasma. The plasma particles scatter off the bubble wall, and if this interaction violates CP, the scattering is different for particles and antiparticles, which will then have different transmission and reflection coefficients. For example, the presence of the CP violating top yukawa coupling eq. (5.2), may lead to an overdensity of left-handed antiparticles over particles in front of the bubble wall (and a compensating overdensity of right-handed particles over antiparticles, as this interaction does not violate baryon number). The EW sphaleron transition only interact with left-handed particles. As there is an overdensity of left-handed antiparticles this will bias the sphaleron rate which destroys antiparticles (in favor of particles as it violates baryon number) over the inverse rate, and a net baryon asymmetry is created.

Left to itself, all the fast plasma interactions would bring the system back to equilibrium, and erase the asymmetry. But there is not time for this to happen as the baryons are swept up by the expanding bubbles. If the PT is strong $v/T \gtrsim 1$ the sphaleron rate eq. (5.7) is suppressed inside the bubble, and the baryons remain. At the end of the PT, when bubbles collide and coalesce, there will be a net baryon number created.

The calculation of the final asymmetry is complicated, because of finite temperature effects (and e.g. the IR contributions of soft photons, as we saw for the calculation of the effective potential), non-equilibrium dynamics, and non-perturbative dynamics. Calculations are usually done in a EFT-like approach, where processes on different timescales are separated. Let's assume the bubble wall background is changing slowly on the time-scales of

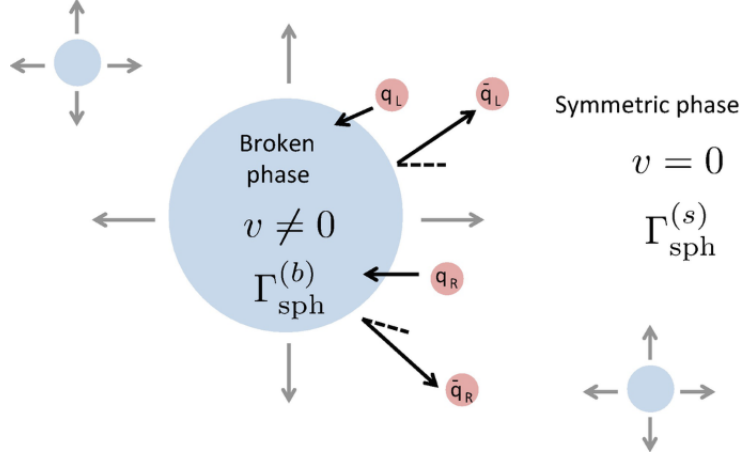


Figure 6. Electroweak baryogenesis mechanism.

the CP-violating plasma interactions, and can be treated as adiabatically changing. The sphaleron transitions are also relatively slow, and the process can be considered as a two step process: first a CP asymmetry is created, and then at a later time this is transferred in a baryon asymmetry. The calculational approach will then be to determine the phase space densities of the plasma particles interacting with the slowly changing bubble wall background.

Consider the distribution function $f(\mathbf{x}, \mathbf{p}, t)$, which is a function of position, proper momentum and time. It describes the density of particles at time t , at the point \mathbf{x} and with momentum \mathbf{p} . (Quantum mechanically no particle can be localized in phase space at a point (\mathbf{x}, \mathbf{p}) , and one should integrate over a (small) phase space volume to get the probability to find a particle in that volume.) Integrating the distribution function over momenta gives the particle number density:

$$n(\mathbf{x}, t) = g_s \int \frac{d^3\mathbf{p}}{(2\pi)^3} f(\mathbf{x}, \mathbf{p}, t) \quad (5.9)$$

with g_s the degeneracy of the species (e.g. spin or polarization states). In a constant background and in thermal equilibrium the phase-space density is space-time independent, and it is the familiar Bose-Einstein and Fermi-Dirac distribution for bosons and fermions $f = (e^{\sqrt{k^2+m^2}/T} \pm 1)^{-1}$. For a system close to thermal equilibrium one can perturb around the equilibrium distributions, and try to solve for the perturbations. The time evolution of the phase space densities is given (at the semi-classical level) by the Boltzmann equations:

$$\frac{df}{dt} = C[f] \quad (5.10)$$

with $C[f]$ the collision term which describes the interaction among the particles. Out of equilibrium both position and momentum are generically a function of time, and the total time derivative can be written as

$$\frac{df}{dt} = \frac{\partial f}{\partial t} + \frac{d\mathbf{x}}{dt} \cdot \nabla_{\mathbf{x}} f + \frac{d\mathbf{p}}{dt} \cdot \nabla_{\mathbf{p}} f = \frac{\partial f}{\partial t} + \mathbf{v} \cdot \nabla_{\mathbf{x}} f + \mathbf{F} \cdot \nabla_{\mathbf{p}} f \quad (5.11)$$

where \mathbf{v} is the particle velocity and \mathbf{F} is the force acting on the particle.

The CP violating yukawa interaction eq. (5.2) gives a complex mass term

$$m(\mathbf{x}, t) = \frac{y_t}{\sqrt{2}} v_b \left(1 + c \frac{v_b^2}{2\Lambda^2}\right) = |m| e^{i\theta} \quad (5.12)$$

with v_b the bubble background: $v_b = 0$ outside the bubble and $v_b = v_N$ at nucleation temperature inside the bubble, and the change in the bubble wall is given by the bounce solution. Taking for simplicity $c = ic_I$ imaginary, then $|m| = \frac{y_t}{\sqrt{2}} v_b$ and $\theta = \frac{c_I}{y_t} \frac{v_b^2}{2\Lambda^2}$ up to higher order corrections in Λ^{-2} . This generates a force when a particle tries to enter the bubble wall, as momentum is needed to generate the mass inside and thus $\dot{p} \neq 0$. For a complex mass this source is different for particles and antiparticles. To calculate the force one needs to find the dispersion relation $E(p)$ in the bubble wall background, which allows to extract the force $\dot{\mathbf{p}}$.

Start with the Dirac equation for the top quark, which can be written as

$$(i\cancel{D} - mP_L - m^*P_R)\psi = 0 \quad (5.13)$$

with $P_{L,R} = \frac{1}{2}(1 \mp \gamma_5)$. Work in the bubble wall rest frame. Consider a large bubble, such that the bubble wall can be approximated as planar, with z the normal direction to the wall. Now decompose the spinor into its chiral components as

$$\psi = \begin{pmatrix} q_L \\ q_R \end{pmatrix} = e^{-i\omega t} \begin{pmatrix} L_s \\ R_s \end{pmatrix} \otimes \chi_s \quad (5.14)$$

These are positive energy solutions, appropriate for particles. Use the chiral basis of

$$\gamma^\mu = \begin{pmatrix} 0 & \sigma^\mu \\ \bar{\sigma}^\mu & 0 \end{pmatrix}, \quad \text{with } \sigma^\mu = (1, \sigma^i) \text{ \& } \bar{\sigma}^\mu = (1, -\sigma^i). \quad (5.15)$$

χ_s is a two component spinor state with $\sigma^3 \chi = s \chi$, and s labeling the spin along the direction of motion, which we take the z -direction. The dirac equation becomes

$$(\omega - is\partial_z)L_s = mR_s, \quad (\omega + is\partial_z)R_s = m^*L_s \quad (5.16)$$

These can be written as uncoupled 2nd order equations

$$\left[(\omega + is\partial_z) \frac{1}{m} (\omega - is\partial_z) - m^* \right] L_s = 0, \quad \left[(\omega - is\partial_z) \frac{1}{m^*} (\omega + is\partial_z) - m \right] R_s = 0 \quad (5.17)$$

For constant m the solution $\omega^2 - k^2 - |m|^2 = 0$ (after Fourier transform $L_s(z) = \int \frac{d^3k}{(2\pi)^3} e^{ikz} L_s(k)$) which is the usual dispersion relation for a free particle. In a spacetime-dependent background (work in the bubble wall rest frame) $p = p(z)$, giving rise to a non-zero force \dot{p} in the dispersion relation; if $m \neq m^*$ the force can be different for the left- and right-handed modes.

To solve the equations, assume the bubble wall background is slowly changing, and use the WKB Ansatz

$$L_s = \omega(z) e^{i \int^z p(z') dz'} \quad (5.18)$$

Substitute in the Dirac equation for L_s , and solve iteratively in a derivative expansion. The solution is

$$p = p_0 + \frac{s\omega + p_0}{2p_0} \theta' + \mathcal{O}(\partial_z^2), \quad p_0 = \text{sign}(p) \sqrt{\omega^2 - |m|^2} \quad \Rightarrow \quad \omega = \sqrt{(p + \theta'/2)^2 + |m|^2} - \frac{1}{2} s \theta' \quad (5.19)$$

For anti-particles can repeat the calculation for negative energy modes. Results is to set $m \rightarrow -m^*$, which changes $\theta' \rightarrow -\theta'$. Finally, to compute the force entering the Boltzman equation we use the Hamilton equation

$$\dot{p} = - \left(\frac{\partial \omega}{\partial z} \right)_p = - \frac{(m^2)^2}{2\omega} + s s_c \frac{(m^2 \theta')'}{2\omega^2} \quad (5.20)$$

with $s_c = \pm 1$ for particles and antiparticles. The first is a CP conserving force term, the same for particles and antiparticles. As it is larger, it is the dominant friction term as the bubble expands in the plasma, and important to find the expansion velocity of the bubble. The 2nd term is the CP-violating force term, that may generate a chiral asymmetry between left-handed particles and antiparticles. The Boltzman equation is a partial differential equation. It can be solved approximately taking moments, to find the net chiral asymmetry.

The final baryon asymmetry is then

$$\frac{dn_B}{dt} \sim N_f \Gamma_{\text{sph}} \mu_{t_L} - c \Gamma_{\text{sph}} \frac{n_b}{T^2} \quad (5.21)$$

The first term converts an overdensity of left-handed (anti)-particles into a baryon asymmetry, note that the chemical potential μ_{q_L} for the left-handed tops is proportional $n_{t_L} - n_{\bar{t}_L}$. The 2nd term is the washout term, the more baryons are created, the more important it becomes. The sphaleron rate $\Gamma_{\text{sph}}(x)$ is only important outside the bubbles, where baryons can be created, and it becomes small inside the bubble where the transitions are shut off. In the bubble wall rest-frame, the frame that the bubble is at rest, one thus should only integrate the above equation in the z -region outside the bubble.

5.3 Constraints from electric dipole moment measurements

In non-relativistic electrodynamics the interaction of a fermion with spin $\mathbf{S} = \frac{1}{2} \boldsymbol{\sigma}$ with an electric and magnetic field is described by the Hamiltonian

$$H = -\mu(\mathbf{S} \cdot \mathbf{B}) - d(\mathbf{S} \cdot \mathbf{E}) \quad (5.22)$$

with μ and d the magnetic and electric dipole moment respectively. Turning on a magnetic (electric) field puts a torque on the system leading to spin precession with angular velocity $\omega = 2\mu|\mathbf{B}| \sin \theta$ ($\omega = 2d|\mathbf{E}| \sin \theta$).

Under a time-reversal $T : t \rightarrow -t$ and parity $P : \mathbf{x} \rightarrow -\mathbf{x}$

$$\begin{aligned} T : & \quad \mathbf{S} \rightarrow -\mathbf{S}, & \quad \mathbf{B} \rightarrow -\mathbf{B}, & \quad \mathbf{E} \rightarrow \mathbf{E}, \\ P : & \quad \mathbf{S} \rightarrow \mathbf{S}, & \quad \mathbf{B} \rightarrow \mathbf{B}, & \quad \mathbf{E} \rightarrow -\mathbf{E}, \end{aligned} \quad (5.23)$$

The transformations of E, B can be deduced from the Lorentz force $\mathbf{F} = m\mathbf{a} = q(\mathbf{E} + \mathbf{v} \times \mathbf{B})$, under T : $\mathbf{a} \rightarrow \mathbf{a}$ and $\mathbf{v} \rightarrow -\mathbf{v}$, while under P : $\mathbf{a} \rightarrow -\mathbf{a}$ and $\mathbf{v} \rightarrow -\mathbf{v}$. Spin behaves just as angular momentum $\mathbf{L} = \mathbf{r} \times \mathbf{p}$. Magnetic dipole moments (MDMs) are invariant under T and P , but electric dipole moments (EDMs) violate both T and P . The CPT theorem tells that T violation is equivalent to CP violation. Hence, measurement of an EDM is a probe of CP violation.

The Dirac Lagrangian for a fermion

$$\mathcal{L} = \bar{\psi} i \not{D} \psi - m \bar{\psi} \psi \quad (5.24)$$

with covariant derivative $D_\mu = \partial_\mu + ieA_\mu$, gives in the non-relativistic limit a MDM with $\mu = eg/(2m)$ and $g = 2$, but no EDM $d = 0$. This can be seen by calculating the tree-level diagram in fig. 7, which is left as an exercise. The absence of an EDM is expected as QED does not violate CP. The MDMs and EDMs get loop level contributions

$$\delta\mathcal{L} = -\frac{1}{2} \bar{\psi} \sigma^{\mu\nu} \left(\frac{ea}{m} + i\gamma^5 d \right) \psi F_{\mu\nu} \quad (5.25)$$

with $a = (g - 2)/2$ the anomalous magnetic moment. In the SM there is CP violation in the CKM matrix (and in the θ -term, which we ignore). Consider the electron. At one loop there are only CP conserving diagrams, see fig. 7, contributing to a but not d . Only at 3 loops is the EDM first generated from CKM-interactions. In SM the electron magnetic and electric dipole moments are

$$\mu_e \simeq 100 \text{ e fm}, \quad d_e \simeq m_d \frac{m_c^2 \alpha_s G_F^2}{108\pi^5} \mathcal{J}_{\text{CP}} \simeq 10^{-21} \text{ e fm}, \quad (5.26)$$

with $\mathcal{J}_{\text{CP}} \simeq 3 \times 10^{-5}$ the Jarlskog invariant. The CKM EDM is really small.

Currently the strongest bound on the electron EDM come from the ACME experiment, which give the constraint $d_e \lesssim 10^{-29} \text{ e cm} = 10^{-16} \text{ e fm}$. The sensitivity is way off to measure the CKM EDM. However, if new CP violating physics exist this can give a dominant contribution to the EDM, and the ACME results are actually a quite powerful constraint. On dimensional grounds a tree-level contribution to the electron EDM by new physics at a scale Λ will be of the order

$$d_e \sim \frac{m_e}{\Lambda^2} e \sim 10^{-23} \left(\frac{\text{TeV}}{\Lambda} \right)^2 \text{ e cm} \leq 10^{-29} \text{ e cm} \quad (5.27)$$

which gives the constraint $\Lambda \gtrsim 10^3 \text{ TeV}$. If the EDM is generated at n -loop level, we expect n loop factors $(4\pi)^2$ (and possibly further suppression by small couplings), reducing the bound on Λ . Still, bounds can be much stronger than currently probed in the LHC;

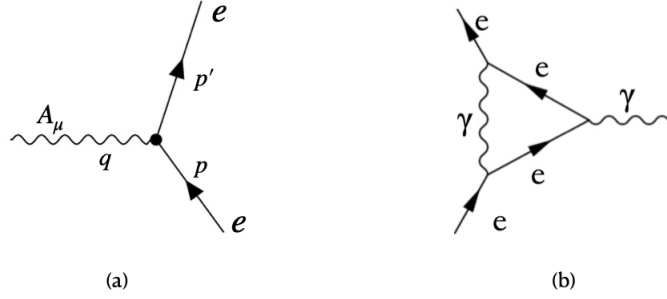


Figure 7. Tree level (a) and one-loop (b) contribution to the magnetic dipole moment of the electron within QED.

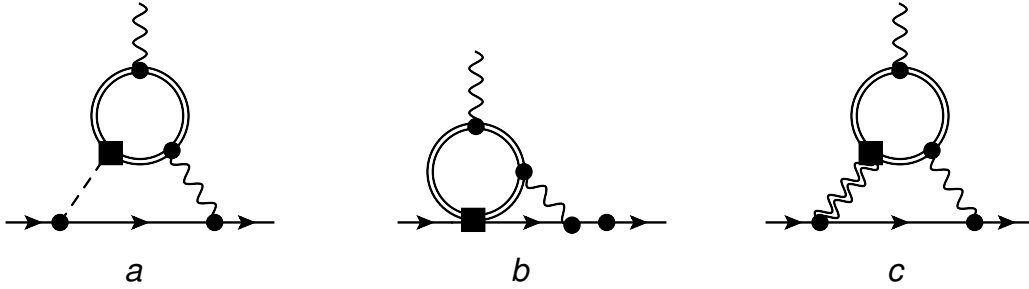


Figure 8. Two-loop diagrams contributing to the electron EDM. Single (double) lines denote the electrons (top quarks), dashed lines the Higgs boson, and wavy single (doubles) lines the photons (Z-bosons). Circles denote SM vertices, while squared denotes CPV dimension-six vertices. Only one topology for each diagram is shown.

If we consider the CP violating correction to the top yukawa coupling that we looked at before eq. (5.2), this generates an EDM at two-loop level, see fig. 8

$$\frac{d_e}{e} = -\frac{8\alpha_{\text{em}}}{(4\pi)^3} m_e N_c Q_t^2 g(x_t) \frac{\text{Im}(c)}{\Lambda^2}, \quad g(x_t) = \frac{x_t}{2} \int_0^1 dx \frac{1}{x(1-x) - x_t} \ln \left(\frac{x(1-x)}{x_t} \right) \quad (5.28)$$

with $x_t = m_t^2/m_h^2$, and numerically the two-loop function is $g(x_t) \approx 1.4$. For $\text{Im}(c) = 1$ this gives the very strong bound $\Lambda \geq 7.1 \text{ TeV}$ on the cutoff scale.

The ACME bound rules out the simplest scenarios for EW baryogenesis, as the CP violation is too small to obtain the observed baryon asymmetry. Solutions are a fine-tuning in the CP violating couplings such that there is a partial cancellation in diagrams contributing to the EDM, thus weakening the ACME bound on the cutoff scale. CP violating couplings to other scalar fields (e.g. the singlet in the doublet-singlet model) are unconstrained by EDM measurements. Yet, another avenue is to consider different mechanism for EW baryogenesis.

E.g. one could consider resonance effects in EW baryogenesis with multiple fermion flavors. Or a set-up where the plasma particles are (temporarily) trapped in the pockets of false vacuum phase (as it cost energy to enter the bubble), increasing their local density.

5.4 Exercises

5.4.1 Exercise: sphaleron rate

Determine the highest temperature for which the sphalerons are in thermal equilibrium.

5.4.2 Exercise: Dirac equation

- [a] Show eq. (5.13).
- [b] Derive eq. (5.19) and eq. (5.20)

5.4.3 Exercise: Magnetic moment of a Dirac fermion

Calculate the MDM from the Dirac Lagrangian in the non-relativistic limit.

- [a] Show that

$$\psi \sim \begin{pmatrix} \chi_s \\ \frac{\boldsymbol{\sigma} \cdot \mathbf{p}}{2m} \chi_s \end{pmatrix} \quad (5.29)$$

is a solution of the non-relativistic Dirac equation.

- [b] Calculate the tree-level diagram fig. 7 (a), and determine μ .

6 Gravitational waves

The Einstein's equations

$$R_{\mu\nu} - \frac{1}{2}Rg_{\mu\nu} = 8\pi G_N T_{\mu\nu} \quad (6.1)$$

describe how spacetime curves in the presence of matter, and how matter moves in a curved spacetime. The curvature tensor and scalar are constructed from the metric, which measures distances

$$ds^2 = g_{\mu\nu} dx^\mu dx^\nu \quad (6.2)$$

with summation over repeated indices implied. In flat spacetime the metric is $g_{\mu\nu} = \eta_{\mu\nu} = \text{diag}(1, -1, -1, -1)$ of Minkowski spacetime, while e.g. in an isotropic and homogeneous expanding universe the metric is the Friedman-Robertson-Walker eq. (A.1). The coupling between the curvature on the lhs and the energy-momentum on the rhs of the Einstein equations is suppressed by $8\pi G_N = 1/M_{\text{P}}^2$. Around most astrophysical objects such as our sun the gravitational field is weak, with curavure radius R^{-2} much smaller than the planck lenght (the exception of strong gravituational fields are black holes, and near the big bang). We can then perturb the metric around the FRW background and linearize the (non-linear) Einstein equations. Any causal mechanism can only produce gravitational waves on subhorizon scales,

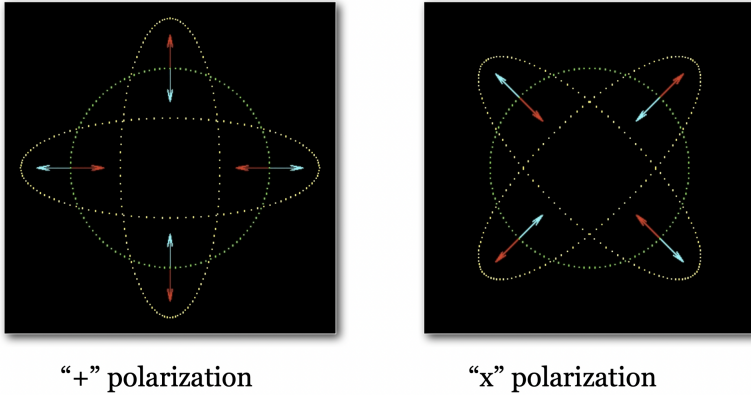


Figure 9. Polarizations for a gravitational wave travelling out of the plane

where curvature effects are small, and for simplicity we neglect the expansion of the universe for now.

Expanding the metric $g_{\mu\nu} = \eta_{\mu\nu} + \tilde{h}_{\mu\nu}$ with $|\tilde{h}_{\mu\nu}| \ll 1$, substituting in Einsteins equations and using Lorentz gauge $\partial^\nu \tilde{h}_{\mu\nu} = 0$ gives

$$\square h_{\mu\nu} = -16\pi G_N T_{\mu\nu} \quad (6.3)$$

with $h_{\mu\nu} = \tilde{h}_{\mu\nu} - \frac{1}{2}\eta_{\mu\nu}\tilde{h}$. The metric is a symmetric 4×4 real tensor, which has 10 dof. The gauge fixing removes 4 dof. The Einstein equation outside the source ($T_{\mu\nu}$) gives 4 constraing equation, which we can use to go to transverse-traceless gauge

$$h_{\mu 0} = 0, \quad h_j^j = 0, \quad h_{ij}^j = 0 \quad (6.4)$$

The first condtion set all temporal components to zero, the 2nd are the the traceless and transverse conditions. In this gauge $\tilde{h}_{\mu\nu} = h_{\mu\nu}$. The existence of the 4 constraint equations can be understood because the Lorentz gauge does not fix gauge invariance fully. There are gauge transformations $x^{\mu'} \rightarrow x^\mu + \xi^\mu$ that leave the lorentz gauge condition invariant, $\tilde{h}'_{\mu\nu} = \tilde{h}_{\mu\nu} - (\xi_{\mu,\nu} + \xi_{\nu,\mu})$ with $\square \xi^\mu = 0$. This additional freedom allows to go to transverse-traceless gauge. The end result is that there are two physical dof, corresponding to the two polarizations. ²

we can use this freedom to impose the transverse traceless conditions):

²This can be compared with electromagnetism where the vector field A^μ has 4 dof, there is one gauge fixing condition e.g. $\partial^\mu A_\mu = 0$, which only partially fixes the gauge as transformations $A^{\mu'} = A^\mu + \partial^\mu \epsilon$ leave the gauge condition invariant for $\square \epsilon = 0$. This additional freedom allows to eliminate another dof, or equivalently, the A_0 equations is non-dynamical and provides a constraint on the system. There are then two physiscal dof (the two polarizations).

In vacuum $T_{\mu\nu} = 0$ eq. (6.3) is a wave equation. If we consider a wave travelling along the z -direction the solution is (in TT gauge)

$$h_{ij}(t, z) = \begin{pmatrix} h_+ & h_\times \\ h_\times & -h_+ \end{pmatrix} \cos(\omega(t - z)) \quad (6.5)$$

with h_+, h_\times the amplitudes of the two polarizations. The gravitational wave travels with the speed of light.

If we put the source term back in we can solve the eq of motion by Green's functions methods $\square_x G(x, x') = \delta^4(x - x')$. We are interested in the retarded Green's functions, such that the solution only depends on past sources and is causal – this is analogous to what is used in electrodynamics. Using that $\nabla^2(1/|\mathbf{x} - \mathbf{x}'|) = -4\pi\delta^3(\mathbf{x} - \mathbf{x}')$ gives

$$\begin{aligned} h_{ij}^{TT} &= \frac{16\pi G_N}{4\pi} \int dt' \int d^3x' \frac{T_{ij}^{TT}(x', t')}{|\mathbf{x} - \mathbf{x}'|} \delta(t' + |\mathbf{x} - \mathbf{x}'| - t) \\ &= \frac{16\pi G_N}{4\pi} \int d^3x' \frac{T_{ij}^{TT}(x', t - |\mathbf{x} - \mathbf{x}'|)}{|\mathbf{x} - \mathbf{x}'|} \end{aligned} \quad (6.6)$$

with T^{TT} the transverse traceless part of the energy-momentum tensor. For an observer far from the source $kr \gg 1$ we can make the approximation $|\mathbf{x} - \mathbf{x}'| = r - \hat{\mathbf{n}} \cdot \mathbf{x}'$ (with $r = |\mathbf{x}|$). We further assume the source is non-relativistic, such that we can neglect internal motions of the source. We can then do a multipole moment expansion in $(\hat{\mathbf{n}} \cdot \mathbf{x}')$. Keeping only the leading order term, this gives

$$h_{ij}^{TT} \approx \frac{16\pi G_N}{4\pi r} \int d^3x T_{ij}^{TT}(x, t - r) \quad (6.7)$$

Finally, using energy momentum conservation $\partial_\mu T^{\mu\nu} = 0$ one can show that $\int d^3x T^{ij} = \frac{1}{2} \frac{\partial^2}{\partial t^2} \int d^3x T^{00} x^i x^j$ and

$$h_{ij}^{TT} \approx \frac{16\pi G_N}{8\pi r} \frac{\partial^2}{\partial t^2} \int d^3x T_{00j}^{TT}(x, t - r) = \frac{16\pi G_N}{8\pi r} \ddot{Q}_{ij} \quad (6.8)$$

with $Q^{ij} = \int d^2x T^{00}(x^i x^j - \frac{1}{3}\delta^{ij}r^2)$ the quadrupole moment, and (for weak fields) $T^{00} = \rho$ the energy density.

If a gravitational wave passes two test particles at rest located at $\mathbf{x} = (0, 0, 0)$ and $\mathbf{x} = (\epsilon, 0, 0)$, the proper distance between them changes as

$$l = \int \sqrt{ds^2} = \int_0^\epsilon \sqrt{|g_{xx}|} dx \simeq (1 + \frac{1}{2}h_{xx}(x=0))\epsilon \quad (6.9)$$

The gravitational wave is curving the spacetime, which we can detect by the geodesic deviation it introduces.

Gravitational waves are generated by accelerated mass distributions with a non-zero quadrupole moment. Spherical system will not produce a gravitational wave signal, as the

quadrupole is zero, but any deviation from spherical symmetry can. Also the system must be accelerating, and a system in stationary motion does not radiate. As the coupling is $8\pi G_N = 1/M_{\text{P}}^2$ suppressed, these sources must be energetic to obtain observable waves, especially if the sources are far away.

6.1 GW from 1st order PT

The energy density in gravitational waves is

$$\rho_{\text{gw}} = \frac{\langle \dot{h}_{ij} \dot{h}_{ij} \rangle}{4\pi} = \int \frac{df}{f} \frac{d\rho_{\text{gw}}}{d \log f} \quad (6.10)$$

with f the frequency, and from now on we set $8\pi G_N = 1$. The superposition of GW produced by a large number of unresolved sources in the early universe form a stochastic background, assumed to be statistically isotropic, stationary and nearly Gaussian. Its main properties are then described by its power spectrum. The quantity that is usually considered to characterize cosmological backgrounds is the spectrum of energy density per logarithmic frequency interval divided by the critical density $\rho_{c,0}$ today

$$h^2 \Omega_{\text{gw}}(f) = \left(\frac{h^2}{\rho_c} \frac{d\rho_{\text{gw}}}{d \log f} \right)_0 \quad (6.11)$$

with $\rho_{c,0} = 3H_0^2$ and $H_0 = 100h \text{ km/s/Mpc.}$, and h parameterizing the uncertainty in today's Hubble constant.

Let's start with an estimate of the typical frequency and signal for a first order PT, which can be sourced by colliding bubbles and plasma waves that are accelerated by the bubbles.

The time of the PT is the nucleation temperature $T_* \approx T_n$. The inverse time duration of the transition is parameterized by $\delta t_*^{-1} = \beta$. For subhorizon causal mechanisms $\beta/H_* > 1$; in the case of a PT this is the requirement that the PT ends and bubbles coalesce. β can be defined from the bubble nucleation rate eq. (4.16) via

$$\beta = - \left. \frac{d(S_3/T)}{dt} \right|_* \simeq \frac{\dot{\Gamma}}{\Gamma} \Rightarrow \frac{\beta}{H_*} = T \left. \frac{d(S_3/T)}{dT} \right|_* \quad (6.12)$$

The bubble wall radius can be estimated $R \sim v_w/\beta$ with v_w the expansion velocity of the bubble. The characteristic wave number of the gravitational wave is then of the order $k_* \sim 1/R = \beta/v_w$, corresponding to a frequency $f_* = k_*/(2\pi)$. The energy density can be estimated from the eom ???. A time-derivate gives a β -factor, and schematically the eom becomes $\beta^2 \dot{h}^2 \sim 2T$, which suggests $\dot{h} \sim 2T/\beta$. Then $\rho_{\text{gw}} \sim \dot{h}^2/(4\pi) \sim T^2/\beta^2$. Setting $T \sim \rho_s$ equal to the energy in the source (released in the PT transition) and dividing by the total (critical) energy density at time of emission this gives $\rho_{\text{gw}}/\rho_c \sim (H_*/\beta)^2 (\rho_s/\rho_c)_*^2$.

To relate the frequency and energy density at emission to what is observed today one has to take the expansion of the universe into account. The energy density in gravity waves decreases as a^{-4} and the frequency of the gravity waves redshifts as a^{-1} , with a the scale

factor. If the universe has expanded adiabatically since the phase transition, the entropy per comoving volume $S = a^3 g_*(T) T^3$ remains constant eq. (A.21), and the ratio of the scale factor at the transition to the scale factor today is

$$\frac{a_*}{a_0} = 8 \times 10^{-17} \left(\frac{100}{g_*} \right)^{1/3} \left(\frac{1 \text{ TeV}}{T_*} \right) \quad (6.13)$$

The frequency today is then

$$f_0 = f_* \frac{a_*}{a_0} \simeq 10^{-2} \frac{1}{v_w} \frac{\beta}{H_*} \frac{T_*}{100 \text{ GeV}} \left(\frac{g_*}{100} \right)^{1/6} \text{ mHz} \quad (6.14)$$

where we used that $H_*^2 = \rho_{\text{rad}}/3 = \pi^2 g_* T_*^4/90$ to write it in terms of the ratio $\beta/H_* > 1$. This falls in the frequency range for LISA which has largest sensitivity in the mHz range.

The GW are produced in the radiation dominated era, but at later times the universe became matter and cosmological constant dominated. Radiation red shifts as

$$\frac{\rho_{\text{rad}}(T_0)}{\rho_{\text{rad}}(T_*)} = \frac{g_*(T_0) T_0^4}{g_*(T_*) T_*^4} = \left(\frac{g_*(T_*)}{g_*(T_0)} \right)^{1/3} \frac{a_*^4}{a_0^4} \Rightarrow \frac{\Omega_{\text{gw}}}{\Omega_{\text{rad}}} = \left(\frac{\rho_{\text{gw}}}{\rho_{\text{rad}}} \right)_0 = \left(\frac{g_*(T_*)}{g_*(T_0)} \right)^{1/3} \left(\frac{\rho_{\text{gw}}}{\rho_{\text{rad}}} \right)_* \quad (6.15)$$

The only difference between the plasma and GW energy densities, is that the former gets slightly heated each time a dof freezes out; this effect is incorporated in the time-dependence of the number of relativistic dof g_* . As the GW are produced during radiation domination $\rho_{\text{rad}}(T_*) = \rho_c(T_*)$ at the time of emission, and we can thus write

$$\Omega_{\text{gw}} = \Omega_{\text{rad}} \left(\frac{g_*(T_*)}{g_*(T_0)} \right)^{1/3} \Omega_{\text{rad}} \left(\frac{\rho_{\text{gw}}}{\rho_c} \right)_* \sim \Omega_{\text{rad}} \left(\frac{g_*(T_*)}{g_*(T_0)} \right)^{1/3} \left(\frac{H_*}{\beta} \right)^2 \left(\frac{\rho_s}{\rho_c} \right)_*^2 \quad (6.16)$$

The energy density in GWs is maximised for small β (but β exceeds unity), and for larger energy release during the PT. Since $h^2 \Omega_{\text{rad}} \simeq 4 \times 10^{-5}$ and within the SM $\left(\frac{g_*(T_*)}{g_*(T_0)} \right)^{1/3} = \mathcal{O}(1)$ a GW signal above the LISA sensitivity of $h^2 \Omega_{\text{gw}} \sim 10^{-12}$ at mHz requires $(H_*/\beta)(\rho_s/\rho_{\text{tot}})_* \gtrsim 10^{-4}$. Detectible signals only arise from slow and very energetic processes.

For a 1st order PT there are three contribution to the source.

- Collisions of bubble walls and (where relevant) shocks in the plasma.
- Sound waves in the plasma after the bubbles have collided but before expansion has dissipated the kinetic energy in the plasma.
- Magnetohydrodynamic (MHD) turbulence in the plasma forming after the bubbles have collided

The stochastic background is the sum of these processes

$$\Omega_{\text{gw}} = \Omega_{\phi} + \Omega_{\text{sw}} + \Omega_{\text{turb}} \quad (6.17)$$

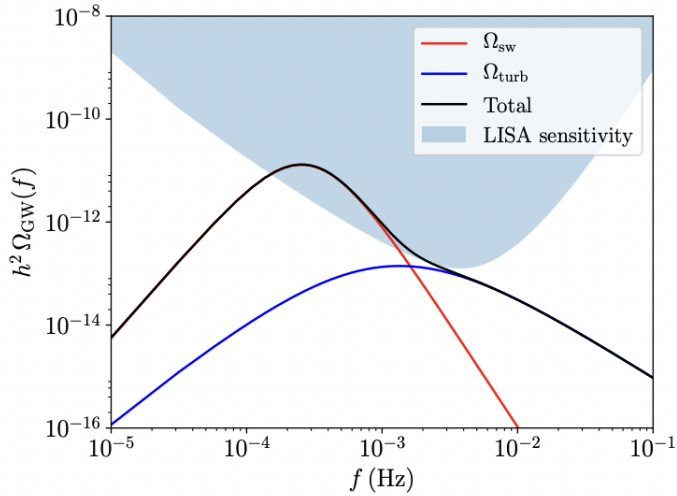


Figure 10. Example of a GW power spectrum for a thermal PT with $v_w = 0.44$, $\alpha = 0.084$, $H_*/\beta = 0.1$ and $T_* = 180$ GeV. The power spectrum is compared to a sensitivity curve obtained for a LISA-like configuration. Taken from 1705.01783.

The bubble wall contribution is generically subdominant, it may only dominate for supercooled/cold transitions, or for runaway bubble walls with a velocity approaching the speed of light – in both cases the transfer of energy to the plasma is small. The plasma will be accelerated and heated by the expanding bubble; the gravitational wave signal will depend on the kinetic energy of the plasma. Hydrodynamica simulations can give more accurate estimates than above. The input is a set of phenomenological parameters describing the system. These are the temperature $T_* \approx T_n$, the bubble wall velocity v_w , and the time-scale of the transition β . In addition, parameters describing the energy content: the ratio of vacuum energy density released in the transition compared to the total energy density in the plasma, and the fraction of vacuum energy density that gets converted into bulk motion of the fluid and into gradient energy of the Higgs field, important to determine the relevant contributions to the total signal.

$$\alpha = \frac{\rho_{\text{vac}}}{\rho_{\text{rad}}}, \quad \kappa_v = \frac{\rho_v}{\rho_{\text{vac}}}, \quad \kappa_\phi = \frac{\rho_\phi}{\rho_{\text{vac}}} \quad (6.18)$$

at the time of emission. Given an actual model, these parameters can then be mapped to the Lagrangian parameters. For β, α this is rather straightforward, but it is much harder to determine the others, as they will depend on the bubble interactions with the plasma.

EW baryogenesis Can the GW signal be used to test models of EW baryogenesis? Unfortunately, this seems hard given sensitivity of upcoming experiments. The GW signal is

largest for strong transition with large, relativistic bubble wall velocities. This maximises the energy that can be transferred to kinetic energy of the plasma, available for GW production.

Baryogenesis on the other hand is most efficient for smaller bubble wall velocities $v_b \sim 0.1$, the efficiency reduces fast for velocities larger than the sound speed in the plasma $c_s = 1/\sqrt{3}$. The reason is that the asymmetry between left-handed particles and antiparticles is created in the bubble wall region where CP is violated. This asymmetry has to diffuse into the symmetric phase, where the sphaleron transition can convert it in a baryon asymmetry. If the bubble wall moves faster than the speed of sound, there is no significant diffusion in the symmetric phase, as the particles are overtaken by the bubble. Sphalerons have ample time to interact, and the baryon asymmetry will be small. This gives an upper bound on the bubble wall velocity for efficient baryogenesis. For very small velocities the system is at all times close to equilibrium and no large asymmetry is produced either.

6.2 Exercises

6.2.1 Exercise: Energy momentum conservation

Show that

$$\int d^3x T^{ij} = \frac{1}{2} \frac{\partial^2}{\partial t^2} \int d^3x T^{00} x^i x^j \quad (6.19)$$

using energy momentum conservation.

A FLRW cosmology

Modern cosmology is grounded on the “cosmological principle”: nobody is at the center of the universe, and the cosmos viewed from any point looks the same as from any other point. It is the Copernican principle – we are not the center of the solar system – taken to the extreme. It implies that the universe (on large scales) is isotropic and homogeneous (as seen by a freely falling observer), and is invariant under spatial translations and rotations. The cosmic microwave background (CMB) and large scale structure surveys confirm the homogeneity and isotropy of the universe on *large scales* > 100 Mpc (the observable patch of our universe is ~ 3000 Mpc).

An isotropic and homogenous universe is described by the Friedman-Robertson-Walker (FRW) metric:

$$ds^2 = -dt^2 + a(t)^2 \left[\frac{dr^2}{(1 - kr^2)} + r^2 (d\theta^2 + \sin^2 \theta d\varphi^2) \right] = g_{\mu\nu} dx^\mu dx^\nu \quad (A.1)$$

with $a(t)$ the time-dependent cosmic scale factor. ds measures the proper distance between two points in spacetime separated by dx^μ . The constant $k = -1, 0, 1$ for an open, flat, or closed universe respectively, corresponding to the 3-dimensional spatial slices being hyperbolic surfaces, flat, or 3-spheres. To write the metric in the above form, the freedom to redefine $r \rightarrow \lambda r$ has been used to normalize $|k| = 1$ for curved universes.

$\{r, \theta, \varphi\}$ are called comoving coordinates, a particle initially at rest in these coordinates remains at rest, i.e. $\{r, \theta, \varphi\}$ remains constant. The physical separation between freely moving particles at $(t, 0)$ and (t, r) is

$$d(r, t) = \int ds = a(t) \int_0^r \frac{dr}{\sqrt{1 - kr^2}} = a(t) \times \begin{cases} \sinh^{-1} r, & k = -1, \\ r, & k = 0, \\ \sin^{-1} r, & k = 1. \end{cases} \quad (\text{A.2})$$

Thus physical distances and wavelengths scale $\lambda \propto a$, and momenta $p \propto a^{-1}$. The distance increases with time in an expanding universe ($\dot{a} > 0$):

$$\dot{d} = \frac{\dot{a}}{a} d \equiv H d, \quad (\text{A.3})$$

with $H(t)$ the Hubble parameter or constant (to indicate it is independent of spacial coordinates). The above is nothing but Hubble's law: galaxies recede from each other with a velocity that is proportional to the distance. Hubble's law is borne out by observations; the present day measured Hubble parameter is $H_0 \sim 70$ km/sec/Mp. A subscript 0 denotes the present day value of the corresponding quantity.

A freely moving particle will eventually come at rest in comoving coordinates as its momentum is red shifted $p \propto a^{-1}$ to zero. The expansion of the universe creates a kind of dynamical friction for everything moving in it. It will be useful to define comoving distance and momenta, with the expansion factored out, via

$$\lambda_{\text{com}} = \lambda_{\text{phys}}/a(t), \quad k_{\text{com}} = a(t)k_{\text{phys}}. \quad (\text{A.4})$$

Motion w.r.t. comoving coordinates is called peculiar motion, it probes the local mass density.

A photon emitted with wavelength λ_{em} from a distant galaxy is red shifted, and observed at present with a longer wavelength λ_0 , given by

$$(1 + z) \equiv \frac{\lambda_{\text{em}}}{\lambda_0} = \frac{a_0(t_0)}{a_{\text{em}}(t_{\text{em}})}, \quad (\text{A.5})$$

that is light with red shift $(1 + z)$ was emitted when the universe was a factor $(1 + z)^{-1}$ smaller. Another way to look at the effects is that from eq. (A.3) photons are red shifted due to the recession velocity of the source.

A.1 Friedmann equation

In general relativity the metric is a dynamical object. The time evolution of the scale factor in eq. (A.1) is governed by Einstein's equations

$$R_{\mu\nu} - \frac{1}{2} R g_{\mu\nu} = 8\pi G_N T_{\mu\nu} \quad (\text{A.6})$$

with R and $R_{\mu\nu}$ the scalar curvature and Ricci curvature tensor respectively, which are both complicated functions of the metric with up to two metric derivatives. We will use units

in which $M_{\text{p}}^2 = (8\pi G_N)^{-1} = 1$. The gravitational field, that is the metric of spacetime, is sourced and curved by matter/energy. The energy-momentum tensor is dictated by isotropy and homogeneity to be of the perfect fluid form $T_{\mu}^{\nu} = \text{diag}(-\rho, p, p, p)$. Then Einstein's equations reduce to two independent equations

$$H^2 \equiv \left(\frac{\dot{a}}{a}\right)^2 = \frac{\rho}{3} - \frac{k}{a^2} \quad (\text{Friedmann eq.}) \quad (\text{A.7})$$

$$\frac{\ddot{a}}{a} = -\frac{1}{6}(\rho + 3p) \quad (\text{Raychaudhuri eq.}) \quad (\text{A.8})$$

The Raychaudhuri equation can also be traded for the continuity equation

$$\dot{\rho} = 3H(\rho + p) \quad (\text{continuity eq.}) \quad (\text{A.9})$$

which encodes energy conservation; it can also be derived from $\nabla_{\nu} T^{\mu\nu} = 0$. Equation (A.9) can be viewed as the 1st law of thermodynamics:

$$dU = -pdV \quad \Rightarrow \quad d(\rho a^3) = -pd(a^3). \quad (\text{A.10})$$

Introduce the equation of state parameter $p \equiv \omega\rho$. Then the continuity equation can be integrated to give

$$\frac{d\rho}{\rho} = -3(1 + \omega)\frac{da}{a} \quad \Rightarrow \quad \rho \propto a^{-3(1+\omega)} \quad (\text{A.11})$$

From eq. (A.7), neglecting the curvature term, it then follows

$$a \propto \begin{cases} t^{2/(3(1+\omega))} & \omega \neq -1 \\ e^{Ht} & \omega = -1 \end{cases} \quad (\text{A.12})$$

This can be derived substituting $a = t^n$ and eq. (A.11) in eq. (A.7), to give $(n/t)^2 = 1/3t^{-3n(1+\omega)}$. This has the solution $n = 2/(3(1 + \omega))$ provided $\omega \neq -1$. For $\omega = -1$ then $\rho = \text{const.}$ and eq. (A.7) has an exponential solution.

The matter in the universe consists of several fluids $T_{\mu}^{\nu} = \sum_i T^{(i)\nu}_{\mu}$, with $i = \{\gamma, M, \Lambda\}$ for radiation, non-relativistic matter and vacuum respectively. If the energy exchange between them is negligible, it follows that all fluids separately satisfy the continuity equation. We can define an equation of state parameter for each fluid separately $p_i = \omega_i \rho_i$.

- Radiation includes all relativistic species, at present only photons (generically, species are relativistic when $m \ll T$). For radiation $\omega_{\text{rad}} = 1/3$ and thus eq. (A.11) gives $\rho_{\text{rad}} \propto a^{-4}$. If the universe is *dominated* by radiation, it follows from eq. (A.12) that the scale factor grows $a \propto t^{1/2}$.
- Matter includes all non-relativistic or cold matter, at present baryons, dark matter and neutrinos. For matter $\omega_{\text{mat}} = 0$ and thus $\rho_{\text{M}} \propto a^{-3}$. If the universe is *dominated* by matter, the scale factor grows $a \propto t^{2/3}$.

- Vacuum energy (a cosmological constant) ρ_Λ with $\omega_\Lambda = -1$ remains constant in time. If it *dominates* the universe $a \propto e^{Ht}$.

Define $\Omega_i = \rho_i/\rho_c$ with $\rho_c = 3H^2$ the critical density. Then the Friedmann equation eq. (A.7) becomes

$$\Omega = \sum_i \Omega_i = 1 + \frac{k}{(aH)^2} \quad (\text{A.13})$$

Thus Ω is larger, equal, or smaller than unity for an open, flat or closed universe respectively. From observations (CMB data, supernovae, large scale structure, lensing, big bang nucleosynthesis(BBN)) we find for the present values

$$\Omega - 1 \cong 0, \quad \Omega_B \cong 0.05, \quad \Omega_{DM} \cong 0.27, \quad \Omega_\gamma \cong 8 \times 10^{-5}, \quad \Omega_\Lambda \cong 0.68 \quad (\text{A.14})$$

with B and DM denoting baryons and dark matter. Visible matter only makes up a very small part.

A.2 Thermal history

A species in thermal equilibrium has a phase space density given by the Bose-Einstein and Fermi-Dirac distributions

$$f(\mathbf{p}) = \frac{1}{\exp(\omega - \mu)/T \mp 1} \quad (\text{A.15})$$

with $\omega = \sqrt{\mathbf{p}^2 + m^2}$ the energy density, μ the chemical potential and the $-$ ($+$) sign is for bosons (fermions). If interactions rates $A+B \leftrightarrow C+D$ is in thermal equilibrium the chemical potentials are related $\mu_A + \mu_B = \mu_C + \mu_D$. The number and energy density are given by

$$n = g \int \frac{d^3p}{(2\pi)^3} f(\mathbf{p}), \quad \rho = g \int \frac{d^3p}{(2\pi)^3} E(\mathbf{p}) f(\mathbf{p}) \quad (\text{A.16})$$

with g the internal degrees of freedom.

For relativistic degrees of freedom $T \gg m$ this gives

$$n = \frac{g}{2\pi^2} T^3 \int \frac{y^2}{e^y \mp 1} dy = \frac{g c_n}{\pi^2} \zeta(3) T^3, \quad \rho = \frac{g}{2\pi^2} T^4 \int \frac{y^3}{e^y \mp 1} dy = \frac{g \pi^2 c_\rho}{30} T^4 \quad (\text{A.17})$$

with $c_n = \{1, \frac{3}{4}\}$ and $c_\rho = \{1, \frac{7}{8}\}$ for bosons and fermions. In the non-relativistic limit $T \ll m$ and neglecting chemical potentials

$$n \simeq g \frac{g}{2\pi^2} e^{-m/T} (2mT)^{3/2} \int x^2 e^{-x} dx = g \left(\frac{mT}{2\pi} \right)^{3/2} e^{-m/T} \quad (\text{A.18})$$

the same for bosons and fermions, and $\rho = mn$.

The radiation energy density can then be written as

$$\rho_r = \frac{\pi^2}{30} g_*(T) T^4, \quad (\text{A.19})$$

with g_* the relativistic dof in thermal equilibrium with the photons . During radiation domination the Hubble constant scales as $H^2 = \rho_r/3 \propto T^4$. Another useful quantity is the entropy density $s = S/\mathcal{V} = (E+p\mathcal{V})/T = (\rho+p)/T$. For a relativistic species $p = \rho/3$ and $s = \frac{4}{3}(\rho/T)$. The total entropy density is

$$s = \frac{2\pi^2}{45} g_{*S}(T) T^3 \quad (\text{A.20})$$

with g_{*S} the dof contributing to the entropy (for species in thermal equilibrium $g_{*S} = g_*$). Entropy conservation implies that

$$S = a^3 s \propto g_{*S}(T) T^3 a^3 = \text{const.} \quad \Rightarrow a \propto (g_{*S} T)^{-1} \quad (\text{A.21})$$

If no number densities are being created/destroyed the ratio $Y_i = n_i/s$ remains constant, and is therefore often used in Boltzmann equations.

Reaction drop out of equilibrium if the interaction rate becomes slow compared to the Hubble constant $\Gamma \lesssim H$, and interactions can no longer keep up with Hubble expansion and less than one scattering in per Hubble time will occur. The interaction rate for particle A in the reaction $A + A \rightarrow X$ can be estimated as $\Gamma \sim n_A \sigma v$ with σ the cross section and v the velocity of incoming particles (for relativistic particles $v = 1$).

References

- [1] J.I. Kapusta and C. Gale, *Finite-temperature field theory: Principles and applications*, Cambridge Monographs on Mathematical Physics, Cambridge University Press (2011), [10.1017/CBO9780511535130](https://doi.org/10.1017/CBO9780511535130).
- [2] M. Laine and A. Vuorinen, *Basics of Thermal Field Theory*, vol. 925, Springer (2016), [10.1007/978-3-319-31933-9](https://doi.org/10.1007/978-3-319-31933-9), [[1701.01554](https://arxiv.org/abs/1701.01554)].
- [3] M. Quiros, *Field theory at finite temperature and phase transitions*, *Acta Phys. Polon. B* **38** (2007) 3661.
- [4] J.M. Cline, *Baryogenesis*, in *Les Houches Summer School - Session 86: Particle Physics and Cosmology: The Fabric of Spacetime*, 9, 2006 [[hep-ph/0609145](https://arxiv.org/abs/hep-ph/0609145)].
- [5] S. Coleman, *Aspects of Symmetry: Selected Erice Lectures*, Cambridge University Press, Cambridge, U.K. (1985), [10.1017/CBO9780511565045](https://doi.org/10.1017/CBO9780511565045).
- [6] S.R. Coleman, *The Fate of the False Vacuum. 1. Semiclassical Theory*, *Phys. Rev. D* **15** (1977) 2929.
- [7] A.D. Linde, *Decay of the False Vacuum at Finite Temperature*, *Nucl. Phys. B* **216** (1983) 421.
- [8] D. Bodeker and W. Buchmuller, *Baryogenesis from the weak scale to the grand unification scale*, *Rev. Mod. Phys.* **93** (2021) 035004 [[2009.07294](https://arxiv.org/abs/2009.07294)].
- [9] A. Riotto, *Theories of baryogenesis*, in *ICTP Summer School in High-Energy Physics and Cosmology*, pp. 326–436, 7, 1998 [[hep-ph/9807454](https://arxiv.org/abs/hep-ph/9807454)].